Universidade de Aveiro Departamento de Química

Ano 2013

Cristiano Pereira Ramos

Ensaios Catalíticos e Modelação da Oligomerização de Olefinas Leves

Catalytic Essays and Modeling of Light Olefins Oligomerization

Universidade de Aveiro
Ano 2013

Departamento de Química

Cristiano Pereira Ramos

Ensaios Catalíticos e Modelação da Oligomerização de Olefinas Leves

Catalytic Essays and Modeling of Light Olefin Oligomerization

Dissertação apresentada à Universidade de Aveiro para cumprimento dos requisitos necessários à obtenção do grau de Mestre em Engenharia Química, realizada sob a orientação científica do Professor Doutor Carlos Manuel Silva, Professor Auxiliar do Departamento de Química da Universidade de Aveiro, e co-orientação do Doutor Zhi Lin, investigador do Laboratório Associado CICECO da Universidade de Aveiro.

Dedico este trabalho aos meus pais e amigos.

o júri

Presidente	Maria Inês Purcell de Portugal Branco Professor Auxiliar e do Departamento de Química da Universidade de Aveiro
Arguente	Doutor Eduardo Luís Gomes Oliveira ISENSIS - I&D em Engenharia Química Lda. - Portugal
Vogais	Prof. Doutor Carlos Manuel Santos Silva Professor Auxiliar do Departamento de Química da Universidade de Aveiro
	Doutor Zhi Lin Investigador do Laboratório Associado CICECO, Departamento de Química da Universidade de Aveiro

Agradecimentos

Em primeiro lugar gostaria de agradecer à Universidade de Aveiro por estes anos que passei, pois foi o local que possibilitou o desenvolvimento das minhas competências.

A orientação do Professor Carlos Silva foi bastante importante para a realização deste trabalho, foi um professor que desde cedo me cativou, pelos seus conselhos, carácter e paixão, ao longo do meu percurso académico. Também ao Dr. Zhi Lin que me deu conselhos importantes em alguns tópicos deste trabalho.

Como não poderia deixar de ser, quero agradecer ao Bruno Antunes, que durante a realização deste trabalho me acompanhou no dia-a-dia. Os seus conhecimentos e sugestões nos mais diversos temas ajudaram-me a tornar este trabalho e este trajeto mais enriquecedor. Também um grande obrigado ao Bruno Figueiredo pelos seus amplos conhecimentos em diversos tópicos, um apoio também por si importante.

Nunca esquecerei também os momentos passados com todos os meus colegas de curso, em especial Nuno Costa e a Sara Silva, que se tornaram companheiros para a vida. Todos eles sabem que foram um grande apoio e uma grande ajuda neste percurso académico.

Por fim, quero agradecer aos meus pais, amigos e à minha querida Ana, pelo seu grande apoio que me deram ao longo deste curso. Em especial à minha mãe que possibilitou tudo isto. Foi tudo de mim, para mim e para vocês. Um grande obrigado!

palavras-chave

Oligomerização, modelação, olefinas leves,1-buteno, H-ZSM-5, catálise heterogénea, diesel.

resumo

Nos últimos anos tem-se observado um aumento da procura de diesel, comparativamente com a gasolina. A produção de gasolina aumentou à custa do aparecimento das unidades de FCC. Deparando com este facto, a produção de diesel tem de acompanhar a sua crescente procura, e essa reposta encontra-se precisamente nestas unidades de FCC. Aquando a formação de gasolina nestas unidades, um dos subprodutos gerados em maior quantidade é a corrente de olefinas leves. As olefinas, na presença de um catalisador, e sujeitas a alta pressão e temperatura formam produtos de elevado valor comercial na gama do diesel.

Nesta dissertação foi estudada, precisamente, a oligomerização de olefinas leves através de ensaios catalíticos. O processo consiste na combinação no mesmo reator, de um catalisador zeolítico a 200ºC com uma alimentação de buteno, acompanhado de um caudal de inerte para diluição do reagente. A oligomerização do 1-buteno permite obter produtos na gama diesel C_{10} a C_{20}.

A instalação experimental foi montada no início da dissertação. Antes da sua utilização, sucessivas correcções a nível de fugas, durante vários ciclos de aquecimento, tiveram de ser efectuadas de modo a deixá-la operacional. Foi utilizada para activação do catalisador, calibração do GC e para a realização da oligomerização de 1-buteno.

Foi utilizado o catalisador zeolítico H-ZSM-5 comercial (Zeolyst CBV 3024E com uma razão Si/Al=15). Este catalisador devido à sua microporosidade e estrutura permite a ocorrência de selectividade de forma, que favorece a formação de produtos lineares.

A instalação foi testada e foram efectuadas experiências a alta pressão (30 bar), tendo sido possível obter produtos na gama do diesel. Estes produtos foram identificados por cromatografia gasosa com um detector FID acoplado.

Um modelo de equilíbrio e cinética foi estudado e programado de modo a prever o comportamento da reacção através da variação do tempo adimensional de reacção, pressão, temperatura e da alimentação.

keywords

Oligomerization, modeling, light olefins, 1-butene, H-ZSM-5, heterogeneous catalysis, diesel.

abstract

In past years it has been observed an increase demand of diesel compared to gasoline. The production of gasoline has increased significantly after the installation of FCC units. During gasoline production, light olefins are obtained as side product. These light olefins, in the presence of a catalyst and submitted to high temperature and pressure, form high commercial products in diesel range.

In this work, 1-butene oligomerization via zeolite catalysis was studied. The process can be conducted in a reactor with an acid catalyst at 200 ℃ with 1-butene diluted in nitrogen (feed) to form products in diesel range (C_{10}-C_{20}).

The experimental set-up was assembled at the beginning of the thesis. Before use, successive leak tests, consisting of heating-cooling cycles, have been performed to leave the equipment operational. The installation is able to carry out the catalyst activation and 1-butene oligomerization.

With respect to the catalyst, commercial H-ZSM-5 (Zeolyst CBV 3024E, Si/Al=15) has been used. This catalyst due its microporosity and its structure provides shape selectivity, which favours the formation of more linear products.

The installation was tested and several runs were performed at high pressure (30 bar), which allowed to obtain diesel range products. Their identification was accomplished by gas chromatography with FID detector.

The modeling of literature data was studied in order to predict the reaction behaviour for distinct sets of reaction time, pressure, temperature and feed concentration.

List of Contents

List of Figures

List of Tables

Nomenclature

List of Symbols

ΔG_{fi}^{o}	Standard Gibbs free energy formation for an isomer group
ΔH_{fi}^{o}	Enthalpy of formation of an isomer group
k_b	Bimolecular rate constant
k_e	Elimination rate constant
k_f	Rate constant of forward reaction
k_p	Propagation rate constant
M_w	Molar mass
n_0	Initial number of moles
n_i	Number of moles of the component i
P^0	Standard Pressure
P_C	Critic pressure
P_r	Reduced pressure
r_i	Fraction of isomer i in the group
r'_j	Net rate
T_C	Critic temperature
T_r	Reduced pressure
V_m	Molar volume
υ_{ij}	Stoichiometric coefficients

ΔG_{fi}	Standard Gibbs free energy of formation of isomer I
C_{10}	Decane
C_{12}	Dodecane
C_{14}	Tetradecane
C_{16}	Hexadecane
C_{18}	Octadecane
C_{20}	Icosane
C_4	1-butene
C_6	Hexane
C_8	Octane
F	Mass flow
FID	Flame Ionization Detector
GC	Gas Chromatograph
M	Catalyst mass
N	Number of steps
P	Pressure
R	Ideal gas constant
T	Temperature
$w\ (\%)$	Weight mass per cent
x_i	Molar fraction of the component i
ρ	Density
T	Adimensionless time
ω	Acentric factor

List of Abbreviations

ASA	Amorphous Silica-Alumina
BPR	Back Pressure Regulator
BTX	Benzene, Toluene and Xylene
COD	Conversion Olefins to Diesel
FCC	Fluid Catalytic Cracking
LCN	Light Cracked Naphtha
LPG	Liquid Petroleum Gas
MFC	Mass Flow Controller
MOGD	Mobil Olefins to Gasoline and Distillate
PREoS	Peng-Robinson Equation of State
RON	Research Octane Number
SPA	Supported Phosphoric Acid
TOS	Time on stream
VOCs	Volatile Organic Compounds
WHSV	Weight Hourly Space Velocity (mass flow/catalyst mass)
ZSM	Zeolite Socony Mobil

Superscripts

0	Standard

Subscripts

0	Initial amount
i	Component i/isomer group
f	Formation

1. General Introduction

1.1 Scope and Objectives

In the past years it has been observed an increase demand of diesel compared to gasoline. Gasoline is produced in FCC units. The production of gasoline has been enhanced by the fact that such units exist in a considerable amount. During the FCC of heavy distillates and other thermal technologies light olefins (C_3-C_6) are formed as side products (Figure 1.1)[1].

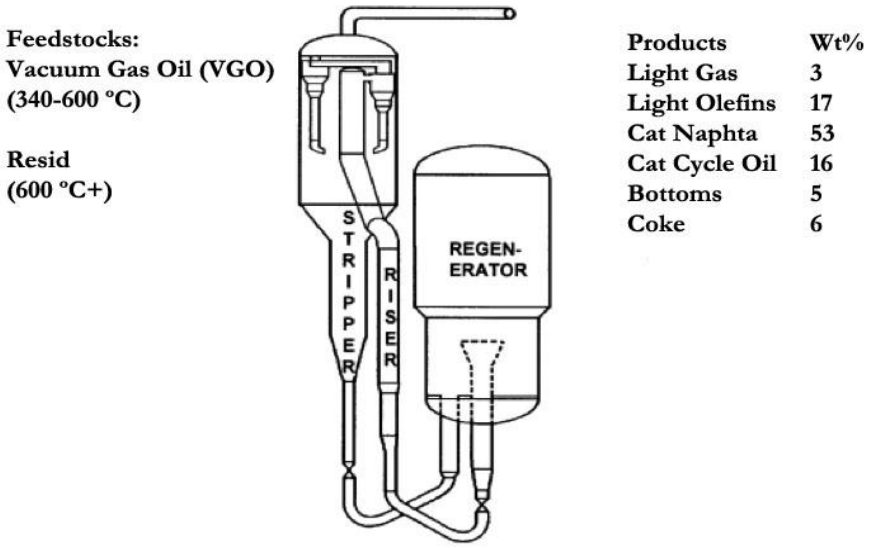

Figure 1.1- Fluid catalytic cracking is a key conversion unit[2].

As the global dieselization trend expands, one of the major problems to be faced by the European refineries is to shift products to meet higher diesel demand associated with lower gasoline demand. While the demand of gasoline is likely to remain stable in US, in Europe the continuous increase of diesel-powered passenger vehicles observed in last years at the expenses of gasoline-powered passenger vehicles has led to a strong surplus of gasoline production compared to middle distillates.

As illustrated in Figure 1.2 although at slower pace, a recent analysis shows that in Europe the increase of diesel demand associated with a lower consumption of gasoline is likely to continue in the future; moreover, there is a strong increase of middle distillate/gasoline ratio along with a slight increase of the total demand between 2010 and 2020. Nowadays the European surplus of gasoline is mainly exported to the US while the shortage of gasoil is compensated by importing from Russia. Along with this trend, environmental awareness is causing a worldwide significant enhancement of fuel quality in order to meet new tighter automotive emission

standards. In these circumstances, European refineries are facing the double problem of increasing the production of diesel and improving its quality. A possible option to increase middle distillate production is to use light olefins for the production of middle distillate through oligomerization[3].

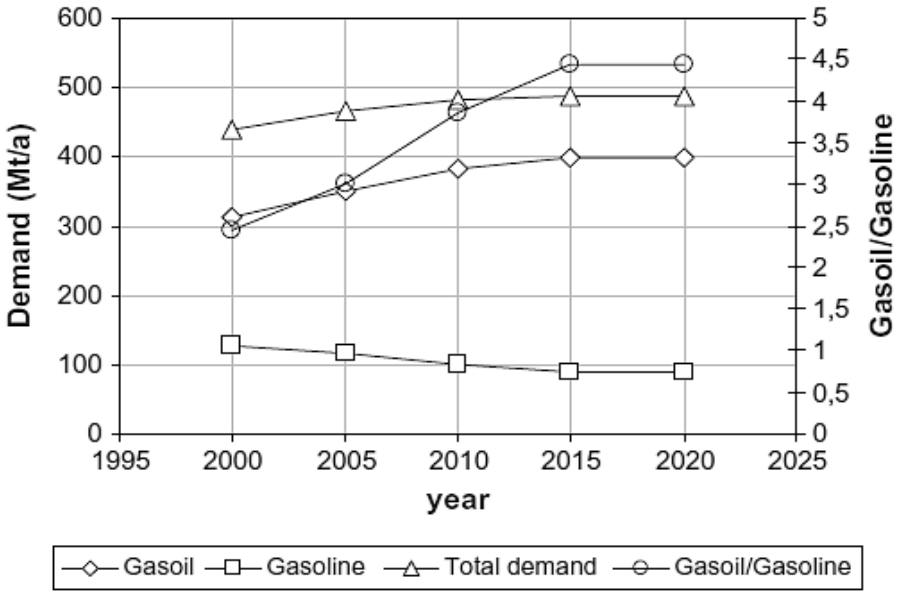

Figure 1.2 - Evolution of EU gasoline and gasoil demand[4].

These side products are a matter of study because they can be used to yield diesel, through oligomerization. The transformation of alkenes over acidic catalysts is a very important reaction with impact on many different applications for the chemical and petrochemical industries. In particular, the catalytic oligomerization of light olefins can be a relevant method to produce hydrocarbons in the gasoline (C_5–C_{10}) and diesel (C_{10}–C_{20}) ranges[5, 6]. Diesel fuel obtained by oligomerization of light olefins has the advantage of the absence of sulfur and aromatics[7].

In the gasoline pool is included pentene, but pentene is associated to VOCs. Volatile organic compounds (VOCs) from evaporative sources are a major source for the generation of the urban ozone. Pentenes are among the lightest, highest vapor pressure components in gasoline, and they have a significant ozone formation potential[8, 9]. Thus, restrictions on light hydrocarbon streams are likely to become more stringent, forcing the lightest components out of the available fuel pool. Therefore, removal of C_5 olefins from gasoline can potentially decrease ozone formation as the C_5 olefins are 4–7 times more active in forming ozone than the corresponding saturated compounds and are among the highest vapor pressure components of gasoline, as mentioned by

Schmidt et al.[10]. A possible approach is to oligomerize light olefins (C_2-C_6), in order to produce oligomers in diesel range.

The acid-catalyzed oligomerization of propylene and butylene was introduced in 1930 as the first commercial catalytic process of the petroleum industry. The product was gasoline-range iso-olefins (C_6-C_{10}) using phosphoric acid impregnated on silica clay, which has been used for several years.

The mechanism of branched alkene oligomerization was studied in the presence of sulfuric acid. Ethylene and propene were, instead, best oligomerized in the presence of phosphoric acid kieselguhr with 60% P_20_5, and became an item of commerce. Because of corrosion problems, other acidic solid catalysts like zeolites were then studied to replace the phosphoric acid-containing catalysts. Also zeolites (where the shape of the product molecules is governed primarily by the pore structure of the zeolite catalyst) have been investigated as catalysts for improving liquid product selectivities in oligomerization of low molecular weight olefins into liquid products. This resulted in a process, MOGD (Mobil olefin to gasoline and distillate), which uses the H-ZSM5 class of zeolites to convert light olefins to higher molecular weight gasoline and diesel[11].

O'Connor has surveyed both homogeneous and heterogeneous catalysis[12] while the reviews of Skupinska[13] and Al-Jarallah et al.[14] focused particularly homogeneous catalysis. Minachev et al. [15] have reviewed their work on the catalytic and physicochemical properties of the zeolites based on pentasils for oligomerizing lower olefins and paraffins into a mixture of aliphatic hydrocarbons of the composition C_6-C_{10} or into a concentrate of aromatic hydrocarbons, depending on the reaction conditions.

The main scope of this work is the oligomerization of light olefins (butene), the stream that can be considered a fuel in petrochemical refinery, while their oligomers can be used for production of diesel fuel, a product with higher commercial value. The process in study and its theoretical basis, as well as recent works are presented in the next chapter. Then, the applied catalysts in study are presented.

2. Light Alkene Oligomerization

2.1 Introduction

The oligomerization of olefins is an important industrial reaction and represents a route to the production of gasoline and diesel fuel-blending stocks, solvent and lubricant stock, plasticizers, dyes, detergents and additives. In particular, oligomerization refers to the preparation of molecules consisting of only a relatively few monomers, in comparison to polymerization which is defined as the production of high molecular weight products. Depending on the number of reacting molecules, and the reaction of the chain growth is called dimerization (n = 2), oligomerization (2 > n > 100), and polymerization (n > 100). Oligomerization occurs in the presence of catalysts, and consists of three steps, initiation, propagation (chain growth), and elimination (hydrogen elimination from β-carbon to the catalytic center)[13]. The terms k_p, and k_e, denote the rate constants for the propagation and elimination reactions, respectively. If k_p, >> k_e, polyolefin will be formed, when k_p<< k_e, dimers are obtained, and finally when $k_p \approx k_e$, oligomers are produced[16].

In propagation step, the olefin monomer C_nH_{2n} oligomerizes to higher molecular weight oligomers $C_{2n}H_{4n}$, $C_{3n}H_{6n}$, $C_{4n}H_{8n}$, etc., while in elimination step, the oligomers so formed can undergo skeletal isomerization, inter-oligomerization (reaction with other oligomers) and cracking via β-scission mechanism with the formation of a mixture of oligomer olefins, not multiple of the monomer. These olefins can in turn oligomerize among them or with the first formed oligomers and so randomize the molecular weight distribution[17].

These oligomer products depend on the catalyst/zeolite porosity, cage size, interconnecting, channel structure, stacking faults, etc. The oligomer chain branching that occurs in oligomerization process is illustrated in Figure 2.1.

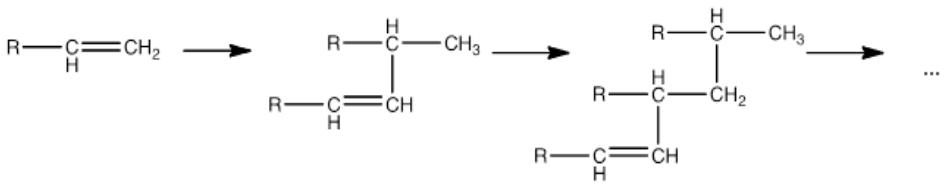

Figure 2.1 - Illustration of the oligomer chain branching [18].

Oligomerization is a reaction for which the activity and selectivity strongly depend on the operating conditions[19]. With different concentration and nature of the acidic catalytic sites, and mainly temperature, oligomeric olefins can undergo various extent of side reactions, such as

coking and hydrogen transfer, leading to the formation of paraffins, cyclo-olefins, alkyl-mono-aromatics and poly-aromatics (Figure 2.2).

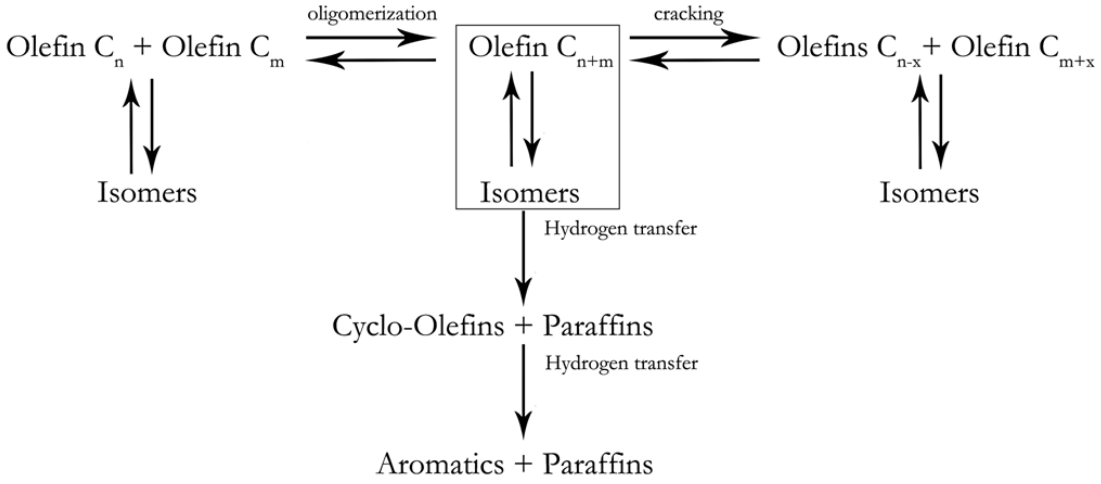

Figure 2.2 - Simplified reaction scheme for oligomerization, cyclization and formation of aromatics[17].

The increase of pressure and residence time inside the reactor leads to higher conversions and average molecular weight of products. The increase of temperature in the lower bound region of the temperature range results in an increase of conversion of olefins and average molecular weight of products whereas a further increase leads to a decrease of average molecular weight caused by the increasing importance of cracking reaction[17]. The influence of temperature and pressure will be discussed further. Another important operating condition of this reaction is the weight hour space velocity (WHSV) defined by:

$$WHSV = \frac{Mass\ Flow\ Rate}{Catalyst\ Mass} = \frac{F}{M} \qquad \textbf{2.1}$$

As reported by Bellussi et al. [17], the conversion of light olefins over H-ZSM-5 decreases when increasing this parameter. The trend of their results, in terms of LCN olefins conversion (per cent weight) in function of time on stream (TOS, h^{-1}), confirms that at higher residence time (i.e. lower WHSV) the system approaches an equilibrium molecular weight distribution. They conclude, in terms of productivity, that at higher space velocity the observed lower material yield is more that rewarded by the higher amount of feedstock processed.

Oligomerization of low molecular weight alkenes leads to the formation of liquid fuel and synthetic lube oils, whereas the high molecular weight alkene oligomerization results particularly in different synthetic lube oils. The unsaturated oligomer products are then hydrogenated to

improve their oxidative stability, or alternatively, are used as feedstocks for various chemical processes using heavy olefins[16].

2.2 Mechanism of Alkene Oligomerization

The acid-catalyzed transformation of alkenes is a classical example of carbenium ion chemistry. Although, the exact nature of the stable intermediate involved in the reaction process is still debatable, the basic steps and sequences of the reaction mechanism were established as early as the 1930s from studies performed using liquid sulfuric acid as catalyst. Transformation of light alkenes in a moderately concentrated acid (<75%) led exclusively to olefinic dimers and trimers produced via the condensation of alkenes followed by the rearrangements of the resulting carbenium ion through hybrid and methyl shifts and, finally, deprotonation. The knowledge gained from *in situ* and *ex situ* studies has established that essentially the same elementary steps are involved in the case of solid acid catalysts such as crystalline or amorphous aluminosilicates. The extent to which individual steps proceeds depends mainly on acid strength, reaction time and, in the case of meso and microporous catalysts, catalyst structure. In addition to gaseous products, the above processes can also generate bulky, immobile, carbonaceous residues, which can poison the active acid sites and become responsible for catalyst deactivation (coke).

The conversion of propene and butene over H-ZSM-5 catalyst has been the focus of considerable attention in the early 1980s. It was proposed that the process is a sequence of oligomerization, cracking and copolymerization reactions[20]. A proposed mechanism for the oligomerization is shown in Appendix A - Figure 8.1, as an example similar in case to any other linear light olefin[21].

The first step involves protonation by the Brønsted acid site. Subsequent monomer addition results in chain growth via carbenium ion. Termination of chain growth can occur as a result of proton transfer, thus regenerating the acid site in the catalyst. The olefinic oligomer molecule thus formed may undergo double bond and skeletal isomerization or disproportionation via carbenium ion intermediate. Olefin cracking may also result in irreversible cyclization and hydrogen transfer reactions, which ultimately result in the formation of cyclo-alkenes, alkyl aromatics and alkanes through conjunct polymerization. The kinetics of these various reactions will determine the ultimate product distribution under process conditions[22, 23].

The oligomerization of propene, 1-decene and isobutene over H-ZSM-5, which had its external surface deactivated using a base molecule, has been studied[24]. The surface-modified H-ZSM-5 produced lower molecular weight and more linear products, indicating that in the absence

of surface-active sites, the oligomerization reaction is of a product shape-selective type. However, the yield was significantly lower than in the case of the unmodified catalyst. In the case of the surface-modified H-ZSM-5, oligomerization occurred inside the zeolite channels and the shape and size of the product molecules were therefore controlled by the space inside those channels and the ability of the product to diffuse in and out of the channels. The relative role of the external surface in determining the product spectrum was also highlighted in a study using different crystal sizes of H-ZSM-22. As the crystal size decreased, i.e. a much greater relative external surface area was available, the activity of the catalyst and the degree of branching of the products increased significantly, as quoted in O'Connor[21].

Oligomerization of n-alkenes over acid solid catalysts can be rationalized in terms of alkyl-carbenium chemistry where the first step is the protonation of the olefin by the Brønsted acid site with formation of secondary alkyl-carbenium ion, followed by either isomerization and/or addition of an alkene molecule. The intermediate so formed can deprotonate and rearrange to a more stable structure. Acid-catalyzed alkene oligomerization can be rationalized by means of carbocation chemistry[13].

The oligomerization of olefins in the presence of zeolites is generally initiated by the Brønsted acid sites[13, 18] and consequently influenced by the important properties of these zeolites including their Brønsted acid site density and acidity, as well as the accessibility of these acid sites. The reaction is done via elementary steps involving carbenium ions [25]. Olefins are protonated on the catalyst and become carbenium ions, which can isomerize to result in new ions with the same carbon atom number, or alkylate to form new ions with higher carbon atom number, or crack to generate new olefins and new ions with a lower carbon atom number.

A cationic mechanism initiated by Lewis or Brønsted acid sites has also been proposed for the oligomerization of olefins[26]. In the first case, a cationic intermediate is formed and the products obtained are mainly branched oligomers (Figure 2.3):

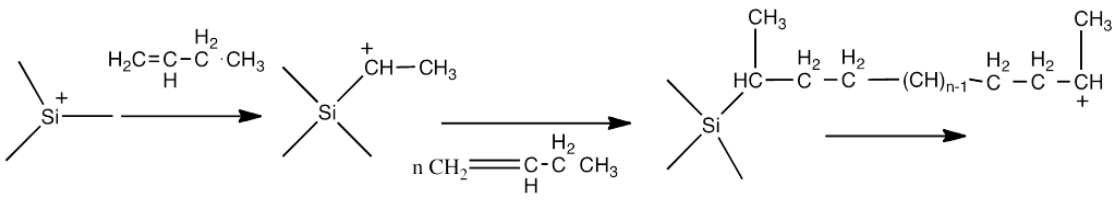

Figure 2.3 - Formation of cationic intermediate and the products obtained.

In the case of Brønsted acidity, two reaction mechanisms have been suggested: the formation of carbenium ion intermediate species (Figure 2.4) which lead to the formation of

branched oligomers [27] and the formation of linear oligomers (Figure 2.5)[26], as mentioned by Corma[7]:

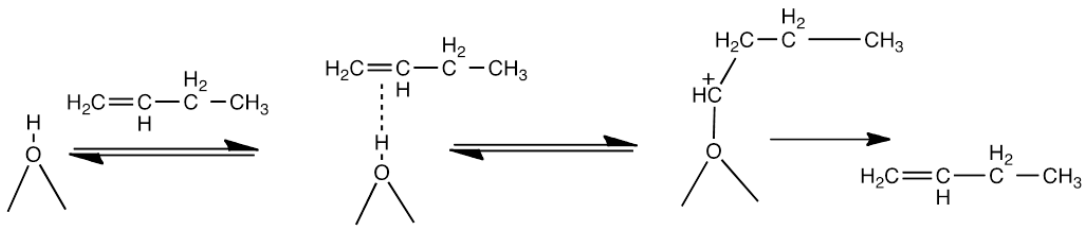

Figure 2.4 - Formation of carbenium ion intermediate and synthesis of branched oligomers.

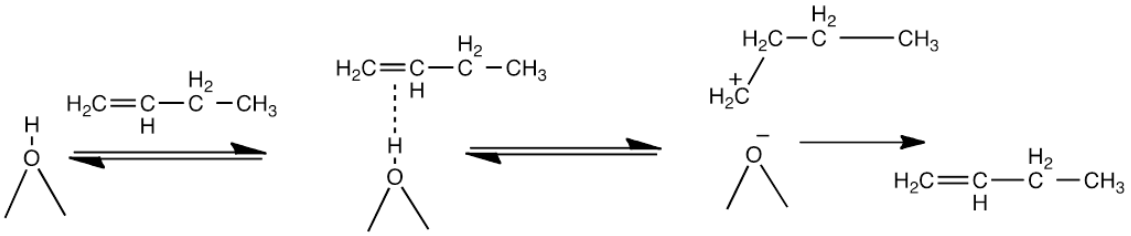

Figure 2.5 – Formation of the same intermediate of Figure 2.4 and the synthesis of linear oligomers.

Theoretically, the reaction is highly exothermic (~ 20 kcal mol^{-1} per double bond) and occurs with a strong reduction of the number of reacting molecules. As a result, from a thermodynamic stand point, oligomerization is promoted by low temperatures and high pressure[17]. Generally, oligomerization is heterogeneously catalysed because catalyst and reactants are in different phases, and the reaction occurs at the interface between phases. The interaction between the reactants and the catalyst surface is a phenomenon of chemical adsorption (or chemisorption) involving the formation of chemical bonds. Chemisorption occurs on coordinatively unsaturated surface ions, which are the active sites. The catalyst surface is not uniform, and the reaction occurs only on specific locations, the active sites.

Heterogeneous catalysts must be prepared with an extensive accessible surface, in order to present the required activity. So, the most important parameters that determine the activity of a given catalyst are its specific surface area and porosity. For porous catalysts, the reactants must diffuse into the pores, and this physical process occurs in parallel with the catalytic reaction. Diffusion limitations will be observed in many situations, especially in the case of large macroporous catalyst particles and small pore sizes. Industrial catalysts can be classified in two groups: catalysts which contain exclusively active species and supported catalysts, when the active species are dispersed results into the support or catalyst carrier.

In addition to the active species and support, catalyst particles may contain stabilizers and binders, in order to improve their mechanical resistance. Thus, heterogeneous catalysis depends on various factors, such as, reaction conditions (temperature, pressure, flow rate) and the nature of catalysts. The catalysts are prepared as particles (spheres, granules, pellets and extrudates) with shape and size determined by the type of reactor used and the physical state of the reactants [28]. With various catalyst nature, they can form a different kind of oligomers depending on the way that the reactants interact with the catalyst surface.

In heterogeneous catalysis, the catalytic action involves the adsorption of reactant molecules on active sites on the surface of the solid catalysts; therefore the transport of those molecules from the fluid phase to the surface, where the catalytic reaction effectively occurs, must be considered in the general mechanism. Similarly, the molecules of the reaction products are eventually desorbed and transferred in outwards direction to the bulk phase. For a porous catalyst, the sequence of steps is described in Figure 2.6 is generally assumed in the case of a generic reaction $A \rightarrow P$, as an example.

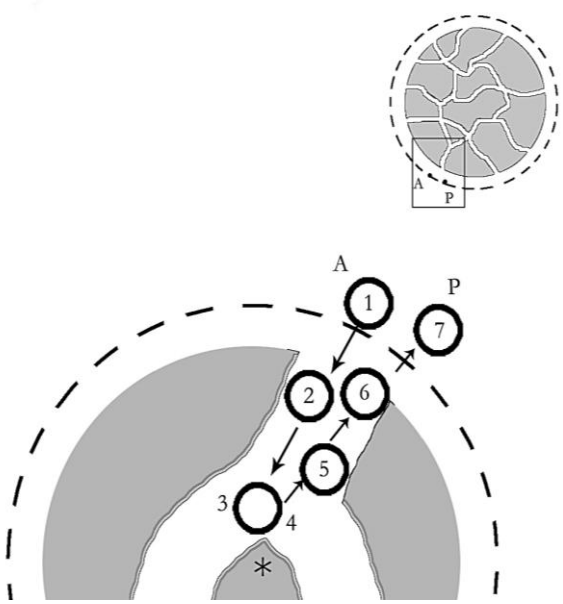

1. Transport of reactants from the fluid phase to the catalyst particle surface (external diffusion – adsorption);
2. Transport of reactants inside catalyst pores (internal diffusion);
3. Adsorption of reactants on the active sites;
4. Surface chemical reaction involving adsorbed species (molecules, atoms);
5. Desorption of products;
6. Transport of the products to the particle surface;
7. Transport of products from the catalyst particle surface to the fluid phase.

Figure 2.6 - General mechanism of the heterogeneous catalytic reaction A→P (* - Active site)[29].

Additionally, in bimolecular reactions, both reactants may adsorb on the catalyst surface or, alternatively, only one of them adsorbs. The products of reaction may also adsorb on the active sites, competing with the reactants [29].

The major groups of heterogeneous catalysts selected for the oligomerization of olefins are acid catalysts (zeolites) and supported nickel catalysts [7]. Practical examples are solid phosphoric

acid (SPA, Ipatieff in 1935), silica-alumina, clays, silica-zirconia and silica-titania, mesoporous silica-alumina, zeolites, organometallic catalysts and sulfonic resins [3, 30] which will be the subject of next topic.

2.3 Catalysts applied in Alkene Oligomerization

Starting from late 50's several works showed the possibility of carrying out the oligomerization on solid acid catalysts such as amorphous silica–alumina, clays, sulfonic resins, silica–zirconia, mesoporous silica–alumina and zeolites.

The catalysts used in oligomerization can be divided in two groups, organics and inorganics. As organics catalysts, acidic ion exchange resins are the most studied, and for the inorganics ones, microporous (zeolites mostly), mesoporous catalysts and other acid-catalysts, such as amorphous silica-alumina (ASA) and SPA are studied. In the next subchapters, recent works on these mentioned catalysts are presented.

2.3.1 Ion Exchange Resins

Resins are organic polymers and the nature and relative quantity of each monomer and also the chain length influence their properties. The incorporation of functional groups, which are responsible for the catalytic activity[31], into the polymeric matrix can be achieved. These functional groups can be not only acidic but also basic, redox or even metallic complexes (transition metals).

Ion exchange resins, particularly the macroporous ones, are versatile catalysts. They have many industrial applications, especially for the production of petrochemicals and solvents. Acid and basic resins have been largely studied for different reactions because their catalytic performance is adequate for numerous applications. The ion exchange resins have been used in different industrial applications over the last decades especially in catalysis[31]. The resin performance depends on recirculation degree, acidity, porosity, size and pore structure, and finally on the specific surface area [32]. Acidic ion-exchange resins are known to be able to catalyze the oligomerization of olefins, e.g. oligomerization of C_4 alkenes over Amberlyst type of resins and oligomerization of higher olefins (C_{10}–C_{32}) over Nafion resin[33]. The oligomers from the C_4 alkenes can be used as diesel fuels. On the other hand, the oligomers of the higher olefins are been used as lubricant, preferably after hydrogenation [34]. The ion exchange resins are catalysts that are regenerative and applied in different hydrocarbon processes. The acidic ion exchange resins, which are available commercially, have different acidic strength, depending on the type of the contained acidic group (e.g.: -SO_3, -COOH). The oligomerization of isobutene was carried out with

different commercial ion exchange resin catalysts. On the studied catalysts they reached different conversions (90-100%), C_{12+} selectivity lower than that of C_8-C_{11}, with the highest value, approximately 30%[1].

Macroporous resins evidence several advantages when compared with homogeneous catalysts, due to the environmental point of view as well as commercial one[35]. The homogeneous catalysts also have low selectivity, and sometimes, secondary reactions occur[36]. In the case of resins selectivity is partially due to matrix effects and good results are generally found. Like other solid catalysts the heterogeneous catalysis with resins permits an easy separation by simple filtration, with subsequent regeneration and reutilization. When resins are used, the generated residues and equipment corrosion are also reduced. These catalysts can also be reused over prolonged period without handling and storing difficulties[37, 38].

The main disadvantage for resin catalysts is their cost, since compared to mineral acids, such as H_2SO_4 and HCl; they are to a large extent more expensive per acid group[31]. Other disadvantage is that resins cannot be calcined for regeneration; generally they are only stable at operation temperatures up to 150 ℃. The initial activity may be recovered by washing with hydrocarbons such as n-butane, but the stability is inferior to the fresh resin without organic residues [37], and for a long-term operation a rapid deactivation is detected in the recovered resin[39]. For a more efficient performance, an easy regeneration of aged catalyst for commercial applications is important, where zeolites are well suited[40].

2.3.2 Microporous Inorganic Catalysts

Facing the difficult to easy regeneration and their cost as high disadvantages, microporous catalysts come out. This class of active catalysts supports a variety of reactions such as cracking, alkylation, aromatization, isomerization of hydrocarbons, etc., owing to their activity, shape selectivity, ion-exchanging properties and specially pore structure, such as the tri-dimensional micro-pore topology and large specific surface area[41]. They suppress all the limitations and disadvantages of the other catalysts, and are assumed the future as catalysts.

Zeolites have been intensively studied in light olefins oligomerization[17, 18, 37, 42-44]. For the zeolite catalysts, the shape of the product molecules is governed primarily by the pore structure of the zeolite catalyst, namely shape and size of the zeolite pores. Many advantages can be gained if a catalyst can be supported on a solid phase without any significant loss in activity. Usually there is insufficient ability in homogeneous catalytic systems to control the extent of oligomerization, and there is also a lack of selectivity to the formation of desired products. Another problem,

which is common to many conventional oligomerization catalysts, lies in the corrosive action of the acids used. In practice, the feedstock for oligomerization of low and/or high molecular weight olefins is usually from some refinery cut, constituting a multi-component system[16].

Zeolite Y is extremely important in heterogeneous catalysis because it is the active component in petroleum refining catalysts for fluid catalytic cracking (FCC process)[45].

In an improved process for the oligomerization of linear, C_{12}-C_{18} olefins, using zeolite catalysis (Y-zeolites) - particularly zeolites with large pores and high Si/Al ratios, the high reactant and product selectivity have been demonstrated with 12-membered ring zeolites useful for the oligomerization of C_{12}-C_{18} terminal and internal olefins. Oligomerization of these unsaturated oligomer products via hydrogenation gives excellent synthetic lubricant base stocks. Internal olefins are generally less reactive than the corresponding alpha-olefins of similar carbon numbers. The lower conversion of longer-chain olefins is likely due to the lower mobility of reactant and product molecules within the zeolite channels. When the olefin substrate is 1-tetradecene, or a mix of C_{13}-C_{16} internal olefins, oligomerization reactivity is higher with the alpha-olefins (alpha olefins > internal olefins), although increasing the reaction temperature can raise the conversion of the C_{13}-C_{14} internal olefins. This work concludes that large pore, ultra-stable, dealuminized Y-zeolites (with high Si/Al ratios) is a very effective solid acid catalysts for C_{12}-C_{18} olefin oligomerization[18].

The shape and size of micropores may induce of shape selectivity. Besides the highly favorable role in providing shape selectivity, the presence of micropores may, in some cases, also limit the catalytic performances of zeolites. Bearing in mind that each zeolite structure can be modified by post synthesis techniques, an almost infinite variety of molecular sieve materials are nowadays at the researcher and engineer's disposal. In many cases, one can tailor zeolites properties for a peculiar and desired application, as mentioned in Ribeiro et. al[46].

With regard to prior research dealing with higher molecular weight olefin oligomerization via zeolite catalysis, medium pore molecular sieves, such as H-ZSM-5 and crystalline metal silicates, are active for the oligomerization of C_{10}-C_{20} 1-alkenes. Oligomerization carried out over H-ZSM-5 zeolite clearly shows that the type and degree of branching are influenced by the pore structure of the catalyst leading to products with lower branching degree where the structure is primarily methyl mono-branched olefin chains[17]. For higher molecular weight, α-olefin oligomerization depends on the amount of catalyst, but does not depend upon the strength of Brønsted and Lewis acid sites. Higher molecular weight α-olefin oligomerization is also known to

be catalyzed by transition metal salts and complexes as well as other homogeneous and heterogeneous Lewis acids[18].

H-ZSM-5 is another example of zeolites, which has gained enormous importance in heterogeneous catalysis. It is industrially used in the synthesis of ethyl benzene, isomerization of xylenes and disproportionation of toluene, and is often considered as the prototype of shape selective catalysts [46, 47], which will be used and reviewed in this work.

2.3.3 Mesoporous Catalysts

Although the major focus of attention over the past 20 years has been on H-ZSM-5, recently there has been significant interest in other classes of catalysts. Eni Technologies [48] has announced the application of amorphous mesoporous silica–alumina catalyst (MSA) as an alternative to the use of supported phosphoric acid. This catalyst is reported to possess good catalytic activity for the oligomerization of light alkenes to gasoline and jet fuel[49-54]. The gasoline boiling range fraction has RON (Research Octane Number) values between 97 and 102 with low benzene contents and the kerosene boiling range has low smoke and freezing point values.

In another study of the oligomerization of butene over a mesoporous aluminosilicate catalyst at 250℃ and pressures in the range of 1.5–2 MPa, it was shown that catalysts with pore openings of approximately 3 nm can exhibit high selectivity and good stability with time for the production of branched dimers. It was suggested that the behavior of these catalysts is related to the moderate strength and high dispersion of the acid sites in the mesoporous structure, as cited by O'Connor et. al[21].

Besides zeolites, mesoporous materials, such as MCM-41, are used, but they have a limitation, which lies on the amorphous wall of the pores. Catani et al. [55] have recently reported the use of mesoporous aluminosilicates (MCM-41) as efficient catalysts for the synthesis of clean diesel fuels. MCM-41 samples with different Si/Al ratios were investigated in the oligomerization of C_2, C_4 and C_5 olefins. While almost no conversion occurred with C_2, very good catalytic performances in terms of activity and selectivity to diesel range were obtained with C_4 and C_5 olefins. An optimum activity and selectivity for catalytic performance was found for a sample with Si/Al ratio of 20. Moreover, catalytic activity was also favored by increasing pressure and contact time. It was found that the presence of small amounts of metal (Ni, Rh or Pt) inside the mesoporous structure did not significantly modify the catalytic activity.

As stated earlier, the porous structure of the acidic catalyst mainly affects the structure of the products. As a general rule it has been observed that branching degree in oligomerization

products increases with the pore size of the acid catalyst. Amorphous Silica–Alumina catalysts (ASA) lead to highly branched products and consequently oligomerization with ASA results in a product with good gasoline octane properties and jet fuel with good cold flow properties. However this class of compounds is not well suited for the production of diesel owing to its poor cetane number[17, 56, 57].

Oligomerization with Supported Phosphoric Acid (SPA) leads to highly branched products with good octane quality therefore is also not suited for the production of diesel cut as confirmed by their very low cetane number. If the process is aimed at maximizing the gasoil yields it is necessary to reach the best tradeoff between cold flow properties and cetane number. In this case, a catalyst showing high shape selectivity (i.e. a zeolite) is more suitable to produce oligomers with a low branching degree and short side alkyl-chains. De Klerk et al. [58] studied the quality of the fuels produced by light alkene oligomerization over SPA and has been shown their dependence on process temperatures and hydration of the catalyst. Hydrogenation of products can, in some cases, dramatically change the octane numbers with respect to the unhydrogenated products. Mantilla et al.[19] investigated an reaction of i-butene on sulfated titania, carried out at temperatures above 200 ℃ , and products range from the dimers (C_8) to higher polymeric olefins (C_{16}). They concluded that the addition of an ‘‘inert’’ diluents to the olefin feed had a positive effect on the stability of the catalyst due to the effect of ‘‘washing’’ of adsorbed high molecular weight olefins deposited on the active sites. On the other hand, solid phosphoric acid has the disadvantage of short lifetime, and it is not possible to tailor the catalyst properties to product demand. Moreover, there are also problems relating to spent catalyst removal from the reactor and the environmental issues related to disposal.

2.3.4 Catalysts Incorporating Metals

Soluble nickel complexes are a most important class of molecular alkene oligomerization catalysts converting, for example, ethene into highly linear l-alkenes with even-numbered oligomers in the C_4–C_{20} range[13, 59]. One of the most important industrial applications of oligomerization uses homogeneous catalysis in which ethene is converted almost with 100% selectivity to 1-butene and n-butenes and then into octenes over a nickel complex.

Supported nickel catalysts are usually prepared by impregnation or ion exchange with supports such as zeolites, silica, alumina or silica–alumina. These catalysts are particularly excellent for alkene dimerization. The molecular weights of the products increase with increasing acid strength. When the acid sites are stronger, broad ranges of hydrocarbons are formed by

oligomerization, cracking, isomerization and hydrogenation. The nature of the active site is not entirely clear. The acidity of the support will mainly affect the extent of secondary cracking reactions[60].

Propene oligomerization leads mainly to the formation of dimers (Table 2.1), whereas ethene produces higher oligomers via an Eley–Rideal mechanism. The use of supported nickel catalysts results in very high conversions at temperatures as low as 80 °C, as opposed to the reaction on SiO_2 –Al_2O_3, which requires a temperature of at least 180 °C [61]. Clay-type structures such as 2:1 layer aluminosilicates, e.g. synthetic mica–montmorillonite (SMM), in which aluminum is substituted for silicon in the tetrahedral layer, produce high yields in the oligomerization of propene at temperatures as low as 150 °C. Various metals such as nickel, cobalt and zinc may be incorporated into the catalyst by ion exchange or by incorporation into the octahedral layer of the framework. Cobalt oxide-on-carbon catalysts produce high yields of dimers when ethene is the feed. At 5 MPa and about 220 °C, heteropoly acids, such as aluminum tungstophosphoric acid, convert alkenes such as propene and butene into middle distillates with no aromatics formation. Results of typical studies are shown in Table 2.1, as quoted by O'Connor et. al [21].

Table 2.1 - Typical product distribution (w %) obtained from propene oligomerization over various acid catalysts. For propene oligomer fractions refer to the carbon numbers: dimer, trimer, tetramer, pentamer and hexamer +. For butene oligomers these correspond to multiples of four[62].

Catalyst	Feed	Reaction T (°C)	Reaction P (MPa)	Weight %				
				Dimer	Trimer	Tetramer	Pentamer	Hexamer
H-ZSM-5	C_3H_6	220	5	18	30	27	14	11
Modernite	C_3H_6	300	5	28	31	23	10	8
Modernite	C_4H_8	250	5	48	40	7	5	-
Solid phosphoric acid	C_4H_8	200	3	9	65	16	10	-
Solid phosphoric acid	C_3H_6	200	3	80	14	6	-	-
SMM[a]	C_3H_6	150	5	9	25	21	21	24
Ni-SMM[a]	C_3H_6	150	5	8	30	26	15	21
SiO_2-Al_2O_3	C_3H_6	200	3	16	35	27	20	2
Ni-SiO_2-Al_2O_3	C_3H_6	80	3	60	22	13	5	-
Amberlyst 15	C_3H_6	130	5	55	30	10	5	-
Aluminium tungstophosphoric acid	C_3H_6	230	5	12	44	25	14	5

[a] SMM: synthetic mica-montmorillonite

2.4 Studied Catalyst: H-ZSM-5 and modifications

Major advantages associated with the use of zeolites are that they can be used over a wide range of temperature, are regenerable and are not environmentally harmful.

In the 1980s, Mobil patented a process using the MFI zeolite H-ZSM-5 to convert light alkenes into hydrocarbon fuels and lubricants[20]. Typical feedstocks used in this process are C_3-C_5 alkenes. The reaction temperatures usually exceed 200 ℃ so as to ensure that the channels of the zeolite catalyst are not blocked by the deposition of heavier oligomers (coke). In addition to oligomerization, this zeolite also catalyzes cyclization and hydrogen transfer reactions, which can result ultimately in the formation of complex product mixtures including aromatics, cyclo-alkanes and alkanes. Among all the zeolitic systems, H-ZSM-5 zeolite has been the catalyst most extensively studied for the oligomerization of light alkenes, and in fact it is the most utilized zeolite, being the catalyst for the commercial MOGD (Mobil Olefins to Gasoline and Distillate) process[63] and COD (Conversion Olefins to Diesel)[17].

Acidity is one of the most important characteristics of zeolites that make them extremely important materials in catalytic applications. The acidity of zeolites is known to depend on several factors: structure, preparation method, chemical composition, impurities, Si/Al ratio, additives and poisons[64]. The stabilities of the catalysts are effectively prolonged by enhancing the Si/Al ratios.

The main feature of H-ZSM-5 (Figure 2.7) is the pore geometry which imposes restrictions on the degree of branching of the product (Products Shape Selectivity), leading to more linear product compared with the products obtained over catalysts with larger pore, as cited by Bellussi et. al[17]. Previously, most of the efforts have been devoted to study oligomerization of C_3 to C_5, considering that C_6^+ olefins can be already used in the gasoline pool.

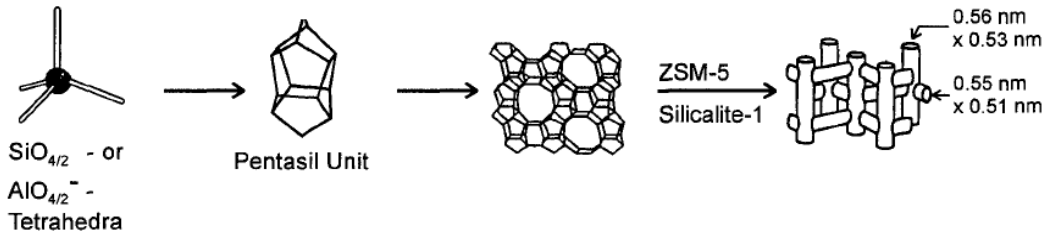

Figure 2.7 - Structure of H-ZSM-5 and their micropore system and dimensions[46].

In order to maximize the diesel fuel yield a H-ZSM-5-based catalyst will be considered. It is widely accepted that Brønsted acid sites inside the channels of H-ZSM-5 are responsible for the

production of linear oligomers, while acid sites existing on the outer surface produced more branched products. Thus, by decreasing the external acidity of H-ZSM-5 zeolite an increase of linear products (with higher viscosity index and higher cetane number) has been observed[7, 24].

Acidic zeolites and, especially, H-ZSM-5 can be used for converting light alkenes into hydrocarbon fuels and lubricants. In H-ZSM-5, the oligomer chains undergo linearization before they can diffuse out of the channels. This zeolite has shown better results than some other catalysts used in oligomerization[6]. The performance of this catalyst for alkene oligomerization was influenced by catalyst synthesis, pre-treatment, and the reaction condition[18].

Martens et al.[65] compared the activity and selectivity of H-ZSM-57 with other medium pore zeolites of different topologies (HZSM-48, HBeta, HFerrierite, HSAPO-11, HZSM-11, HZSM-22, HMCM-22 and H-ZSM-5). It was found that H-ZSM-57 gave a butene conversion of 89% at 80 ℃, while with the other zeolites higher temperatures of 80-180 ℃ were necessary to achieve similar conversions.

Belussi et al.[17] have reported the results of a study aimed at evaluating the use of LCN (Light Cracked Naphtha), through oligomerization with H-ZSM-5-based catalysts, for the production of middle distillates. The conversion of light olefins over H-ZSM5 decreases when increasing the space velocity, whereas lower values don't lead to any significant changes. The results presented are focused on the effect of weight hour space velocity (WHSV) over catalyst deactivation and products quality. This research confirms that the consecutive inter-oligomerization of low molecular weight oligomers is low when deactivation of the catalyst occurs, probably caused by pore plugging due to the progressive accumulation of high molecular weight products in pores (coking). Nevertheless in the practice, in order to keep constant the gasoil quality stable, the reduced activity is balanced by means of a progressive increasing of the reaction temperature, to a limited extent.

The effect of H-ZSM-5 zeolite modification on the selectivity to favorable products can be studied considering various approaches. Brønsted acid centers are generally the catalytically active sites of H-zeolites. By steaming or acid extraction, part of the zeolite can be dissolved or restructured leaving a mesoporous system in addition to the microporous one, which may be of importance in the transport of reactants and products and thus the conversion of relatively large molecules which may be present in the feedstock.

The strength of the Brønsted sites depends on the interaction between the proton and the zeolitic framework or the environment of the framework Aluminium (Al). A completely isolated Al tetrahedron will create the strongest Brønsted acid site. The two main parameters governing the

acid strength of the Brønsted sites are the structural characteristics of the zeolite and its chemical composition. The structural characteristic of the zeolite is related to the proton ability that depends on the T-O-T angle formed between the two adjacent tetrahedral T where the oxygen carries the proton. Lewis acid sites are related to the formation of positively charged oxide clusters or ions within the porous structures of the zeolites. In general, the presence of Lewis acid sites could increase the strength of the nearby Brønsted acid sites, due to an inductive or a synergistic effect between the Brønsted and the Lewis acid sites. The modification of H-ZSM-5 zeolite catalysts with the elements which enhance the surface basicity decreases the readsorption of the basic compounds of the cracking products, such as ethylene, propylene, and butenes, and this is apparently the major cause of the lower aromatics and higher light olefin formation. The alkali treatment of zeolites significantly changes their acidity and pore structure because silica and alumina of the framework are dissolved in alkaline solution. The dissolution of alumina removes aluminum atoms from the zeolite framework; thus, results in the loss of strong acid sites and destruction of zeolite structure. Weak alkali solutions dissolve a small amount of silica and alumina, so create mesopores by enlarging the micropores of zeolites, while strong alkali solutions destroy their crystal structure[41].

H-ZSM-5 modifications

Since the beginning of the studies on H-ZSM-5, different works have been made with modifications, to test their textural properties, their effect on products range, catalyst activity, number of acid sites, etc.

Alkali modified zeolites, usually Na and K, are not recommended by some authors, because of their deactivating effect in most of the catalytic reactions and hydrocarbon transformations. The alkali treatment is not effective in enhancing the overall selectivity to alkenes, but the selectivity for propylene is high because of the rapid elution of primary cracking products. On the contrary, it was observed that the loss of strong acid sites due to alkali treatment suppresses the production of longer alkanes such as hexane and heptanes by reducing further oligomerization[66]. Wang et al.[67] deduced that the role of K is to enhance the dehydrogenation activity of the catalysts and minimize the bimolecular hydrogen transfer reaction, which is responsible for the saturation of small olefins and the formation of products with less aromatics.

Metals induce the dehydrogenating properties of the material whereas acid sites are responsible for the oligomerization of the dehydrogenation products (bifunctional mechanism). By investigating the yield of light olefins versus the Si/Al ratios of catalysts[68-72], it was concluded

that when Si/Al ratio increases the yield of BTX (Benzene, Toluene and Xylene) decreases over the modified H-ZSM-5 zeolites. Higher Si/Al ratios delay the bimolecular hydrogen transfer reactions.

The important job in designing a catalyst is to optimize the balance between the number/strength of acid sites and the type/amount of metals in the modified H-ZSM-5 for maximization of alkene oligomers with relatively low coke formation and catalyst stability. This stability depends on the local structure of the Brønsted acid site and the Si/Al ratio of the zeolite framework. Higher Si/Al ratio of zeolite decelerates the hydride transfer reactions. The reported results indicate that Co, Cu, Zn, and Ag loaded sites on H-ZSM-5 zeolites accelerate the dehydrogenative cracking [73] and cyclo-dehydrogenation reaction.

Rare earth (RE) cations such as La^{3+} and Ce^{3+} have been successfully employed in FCC (Rare earth zeolite Y (REY) catalysts) to improve the ability of the catalyst to withstand high temperature (near 200℃), leading to the increase of catalytic stability, activity and gasoline selectivity[74]. A higher concentration of acid sites has been found in the rare earth exchanged catalyst due to the inhibition of the dealumination of the zeolite; consequently, both the activity and the hydrothermal stability of the catalyst have been improved. They shift the cracking selectivity due to the reduction of hydrogen transfer to produce higher percentages of olefins, which will increase gasoline octane number. On the other hand, as a result of more active sites, both the primary cracking and hydrogen transfer reactions that occur within the zeolite are enhanced[75]. However, the influence of RE modification on the catalytic performances of H-ZSM-5 zeolite is debatable. Some researchers have reported that the introduction of a rare earth metal ion into H-ZSM-5 has a negative impact on its acidic properties[70, 76]. Hartford et al.[76] observed that lanthanium exchanged H-ZSM-5 zeolite has lower number of strong acid sites and higher number of weak acid sites. It neither reduces the effective free pore volume nor enlarges steric hindrances for the passage of linear molecules through the pores of the catalyst.

The modification of H-ZSM-5 zeolite with phosphorus decreases Brønsted acidity[77]; and/or converts strong Brønsted acid sites of H-ZSM-5 into weak Brønsted acid sites that increase the density of the weak Brønsted acid sites without changing the overall acid–base properties. The incorporated phosphorous species are responsible for both the enhanced acid stability and the significantly improved catalytic performance in the cracking of C_4 olefin to propylene and ethylene. Zhao et al.[78] got similar results that the P-impregnated H-ZSM-5 zeolites improve the propylene selectivity greatly and result in excellent anti-coking ability.

In conclusion, the promoter controls the pore characteristics and shape-selectivity zeolite, as well as the acidity of H-ZSM-5, influencing the catalyst activity and hydrothermal stability.

Alkaline and rare earth cations not only increase the surface basicity that reduces the re-adsorption of the basic compounds of the cracking products, such as ethylene, propylene, and butenes, but also enhance the dehydrogenation reaction, which results in light olefin formation. Transition metals alter the acid site distribution, i.e., the ratio of L/B (Lewis/Brønsted acid sites), regulate the concentration, and amend the strength of Brønsted acid sites. The role of Lewis acid sites in accelerating the dehydrogenation reaction combined to a synergistic effect that exists between the Brønsted and the Lewis acid sites, hinder the hydrogen transfer reaction, and improve the dehydrogenative cracking that consequently improve the yield of light olefins. Rare earth ions not only amend the acid strength and distribution but also enhance the surface basicity of H-ZSM-5 catalyst. The modification of H-ZSM-5 with phosphorus is the best compromise in terms of both improving the hydrothermal stability and adjusting the zeolite chemical properties. The higher Si/Al (>80) ratios in H-ZSM-5 framework are beneficial because of the well-established impact of low Al content on limiting the extent of aluminum extraction from the framework structure[79] and thus, increasing the stability of the crystal lattice[80, 81]. Moreover, the higher Si/Al ratios hinder the bimolecular reactions and prevent from the formation of BTX as it is reviewed extensively[41].

3. Experimental Section

3.1 Introduction

With the increase of diesel demand in Europe, associated with a decrease of middle distillate/gasoline production ratio, there was need to face the double problem of increasing the production of diesel and improving its quality. A possible option is to use light olefins for the production of middle distillate through oligomerization[3].

These side products was been a matter of subject because they can be used to yield diesel, through the process of oligomerization. So, this experimental work focuses on this field.

For these experiments a installation was required to perform the catalytic tests, so the choice fell on a tubular reactor.

3.2 Materials, Reagents and Equipment

The reactants, gases, materials and equipment used in this work are described in this section.

Reagents: 1-butene with purity of 99.6% (Praxair); Pure compounds for GC calibration - pentane, hexane, heptane, octane, o-xylene, p-xylene, toluene, nonane, provided from GALP; ASTM D2887 (Sigma-Aldrich) Quantitative Calibration Mix (for GC) of n-Hexane, n-Heptane, n-Octane, n-Nonane, n-Decane, n-Undecane, n-Dodecane, n-Tetradecane, n-Hexadecane, n-Octadecane, n-Eicosane, n-Tetracosane, n-Octacosane, n-Dotriacontane, n-Hexatriacontane, n-Tetracontane, n-Tetratetracontane[82] .

Gases: Air (Oxygen), N_2 (Nitrogen), H_2 (Hydrogen) and He (Helium), all acquired from Praxair.

Materials: Ammonium H-ZSM-5 powder acquired from Zeolyst Products (CBV 3024E) with Si/Al ratio of 30 and surface area of 405 m^2/g [83].

Equipment: Quartz wool discs (16 mm diameter and 5mm thickness) from Elemental Microanalysis [84]; Glass wool, provided from TermoLab; Mass Flow Controller - Bronkhorst EL-FLOW model F-201CV [85]; Chemyx Syringe Pump Nexus 6000 (in a flow rate range of 0.00001µl/min to 200ml/min; pressure up to 68.7 bar, stainless steel syringe with 20mL and 19.13 mm diameter) [86]; Tube Furnace (TermoLab); Equilibar Back Pressure Regulator GS Series [87]; Master GC Fast Gas Chromatography equipped with a FID detector with a split/sliptess injector [88], Teflon and combustible gas detector (TIF8800A)[89] .

3.3 Characterization of H-ZSM-5 catalyst

The samples of NH_3-H-ZSM-5 powder were placed in oven at 120 ℃ during the night to dry. Then, the samples were calcined in furnace at 5℃/min ratio and at 550℃ for 300 min in static air conditions to remove any organic coumpounds and obtain the protonated form and enhance and activate the acidic properties.

The catalyst samples were analyzed by Scanning Electron Microscopy (SEM), X-Ray Energy Dispersive Spectroscopy (EDS) and X-Ray Diffraction (XRD). SEM was performed to evaluate crystallite size and morphology of the H-ZSM-5 catalyst and EDS was used to get Si/Al ratio. They were carried out on scanning electron microscope Hitachi S4100 with Römteck EDS system.

Powder X-ray diffraction (determined by Philips X'Pert MPD) was used to determine the materials framework type and the identification of extra-crystalline phases. Samples were analyzed before and after calcination. The instrument was equipped with an image plate detector and a 45 mV/40 mA at 25℃ generator using Cu-Kα radiation with a wavelength of 1.54 Å.

3.4 Experimental Set-up and procedure

In this study, the butene in liquefied state was obtained by a hook tube system bottle, the butene where is pulled into the tubing and filled a syringe. The feedstock consists mainly in a 1-butene (C_4H_8) diluted. The butene was oligomerized in a fixed-bed down flow reactor equipped with a backpressure regulator. The catalyst was supported with one quartz wool disc, one glass wool disc, with equal dimensions, at the bottom, and another quartz wool above to form a uniformized bed inside the reactor. The catalyst was activated in the reactor at 500 ℃ for 30 min in pure flowing nitrogen before the reaction.

The products were analyzed by a gas chromatograph (GC) equipped with a flame ionization detector (FID) and an VB-1 capillary column with normal paraffins as reference.

3.4.1 Set-up

The experimental equipment used includes in a syringe pump that was choosen by its pressure and fill rate ranges, which are consistent with the desired conditions that will be used. An MFC controls the inert carrier (N_2) flow rate. A mantle temperature was used to control the heating of the reactor. A tubular reactor (1.6 cm internal diameter and 40 cm length) was chosen because of their properties, mainly in their advatanges in ease use, construction, lower cost, fluid-catalyst contact, temperature control, as shown in Appendix B1 - Table 8.1, in grey. The inside of the reactor comprises steel spiral cilinders to promote the heat transfer and mixture of reactants.

The line in and line out of the reactor are heated and properly isolated to avoid heat losses. After the line out, a filter was installed to retain possible catalyst powder, other impurities and wool material, pulled from the reactor. This prevents the contamination on the lines of the box section and the final product. This sector is where the mixture of the products is dragged to the trap at desired conditions. In this installation section, glass wool was used as insulator, to avoid heat losses and provide constant temperature in all section. A picture was taken showing the glass wool inside in the box (Figure 3.1). The liquid products are traped in a cooler vessel and the gas products are analyzed online during the reaction by loading samples into eleven loops available in GC. The experimental set-up is shown in Figure 3.2.

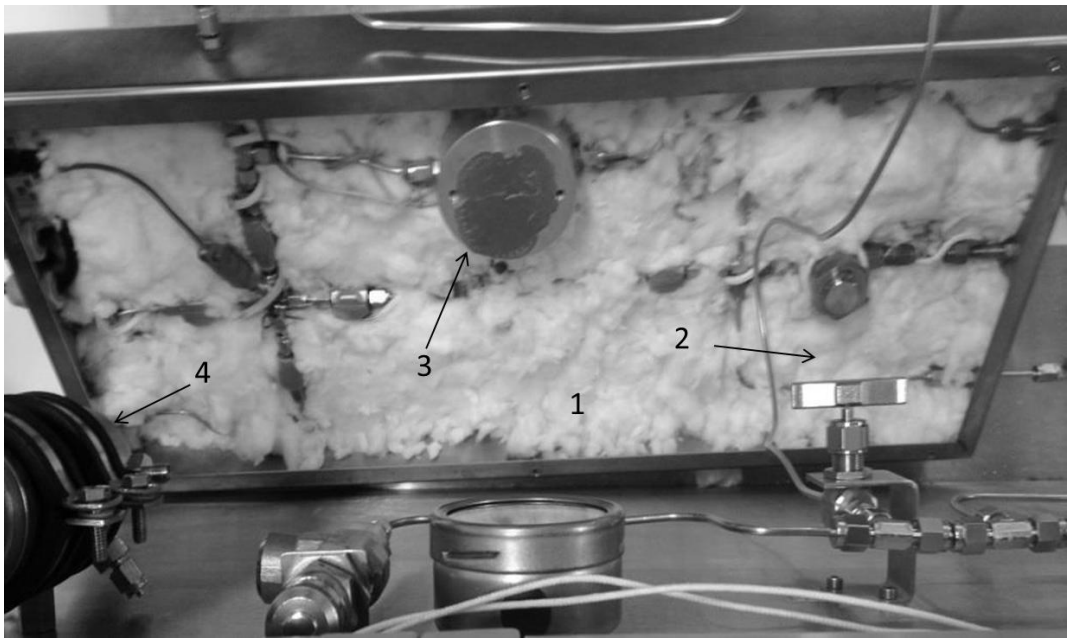

Figure 3.1 - Box section with isolation: 1) Glass wool; 2) Filter; 3) BPR; 4) Manual BPR.

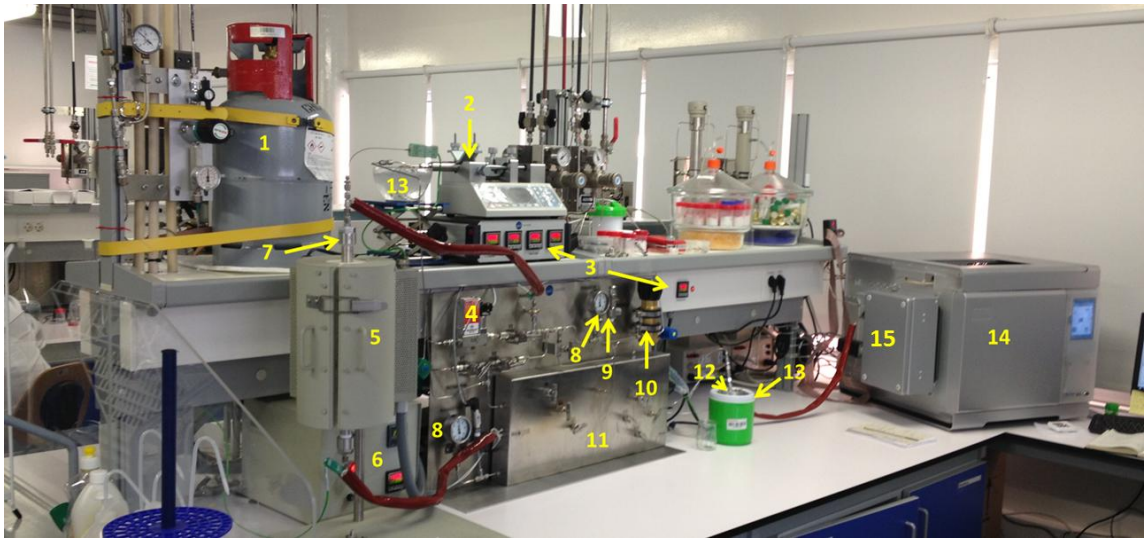

Figure 3.2 - Components of the catalytic apparatus for butene oligomerization: 1) Butene bottle; 2) Syringe pump (Chemyx N6000); 3) Temperature controllers; 4) MFC (Mass Flow Controller - F-201CV) for N_2; 5) Heating tubular oven; 6) Oven temperature controller; 7) Plug Flow Reactor; 8) Manometer(s); 9) Relief valve; 10) BPR (Back Pressure Regulator); 11) Box section of Figure 3.1; 12) Trap; 13) Ice Bath containers; 14) Master GC (DANI - Fast Gas Chromatography); 15) GC injector and load valves container.

3.4.2 Experimental Procedure

This section describes several tests made to plan the appropriate experimental procedure. In Figure 3.3 it is shown the schematic drawing of the installation and respective numbered valves. The heated lines are represented in red; the box section (also shown in Figure 3.1) and the BPR are also heated. This installation allows the catalytic reaction to be performed at different conditions, from high pressure (from 30 bar) to atmospheric pressure and wide temperature range (at 200 °C). The different modes of operation can be consulted in Appendix C – Different modes of the installation operation, in Figure 8.2-Figure 8.5.

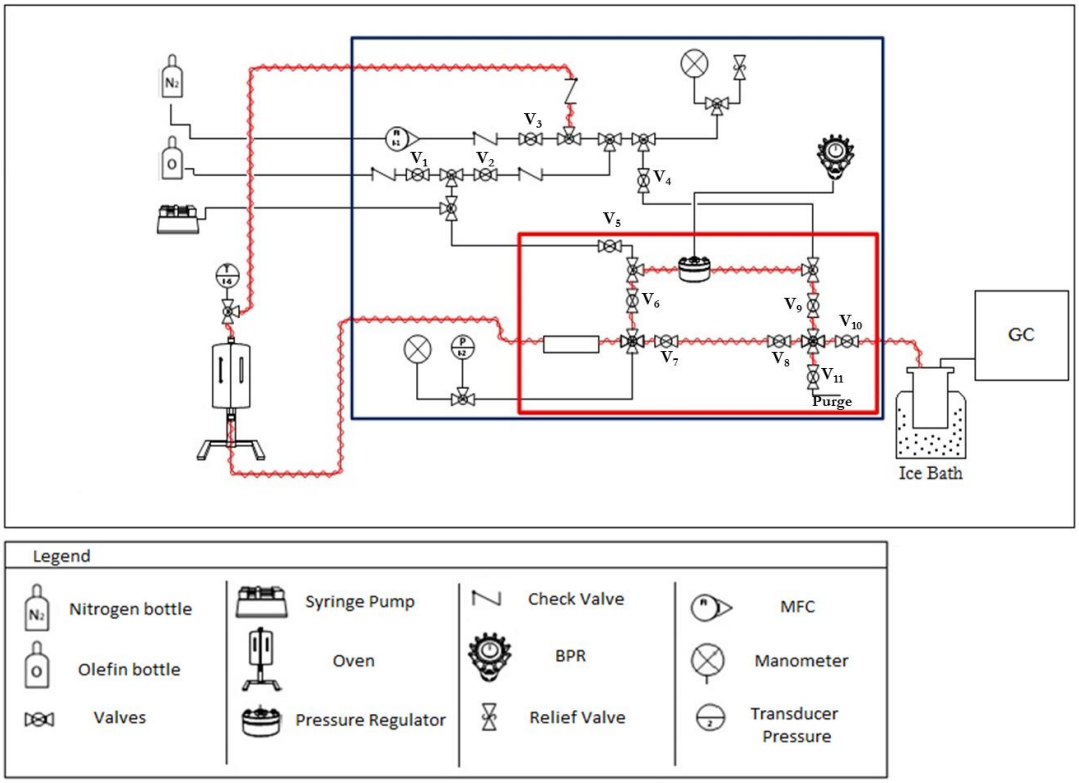

Figure 3.3 - Schematic drawing of the installation presented in Figure 3.2.

Leak Tests

After the system was set up, preliminary tests showed the lack of pressure stability. The pressure was increased up till 30 bar with nitrogen. However, the pressure failed to stabilize. Because butene is a flammable gas, it was used to locate the leaks with the help of combustible gas detector (TIF8800A[89]) and the tubing was tightened. The major problems found were inside the box section, which lead us to disconnect it from the installation. Because after every heating cycle performed at high pressure, the junctions of the tubes and valves have dilated and their subsequent tightening was necessary, this procedure was performed several times until all issues were properly solved. After this section was fixed, problems arose in the grip of the reactor. Several tests using heating cycles and high pressure (nearby 30 bar) indicated that the reactor needed to be well tightened and well isolated, and this could be done by using more teflon layers in the screws of both ends.

Once this problem was solved, the equipment was finally set to begin the experiments. However, to avoid future leaks and because this work involves high temperature (range of 200 °C) and flammable gases, before each experiment, a high-pressure test (50 bar) was always performed. Since the catalyst was already charged in the reactor the tests were executed using only N_2. The operating temperature was approximately 200 °C. If this test was not performed at

this temperature, it might occur the inflammation of leaked alkene during the experiments. For safety purposes the system is equipped with a relief valve. The safety valve operates by releasing a volume of fluid from the system when predetermined maximum pressure is reached (approximately 55 bar at maximum). It prevents the system to overtake the maximum pressure and avoid damaging the equipment, laboratory and personnel.

H-ZSM-5 Activation

The required mass of catalyst was loaded in the reactor in powder form as received and was packed between two quartz wool discs supported in stainless steel cylinders to form a fixed bed. These cylinders present helical cracks to provide the fluid passage, shown in Figure 3.4. The bed is schemetically represented in Figure 3.5.

Figure 3.4 - Stainless steel cylinders.

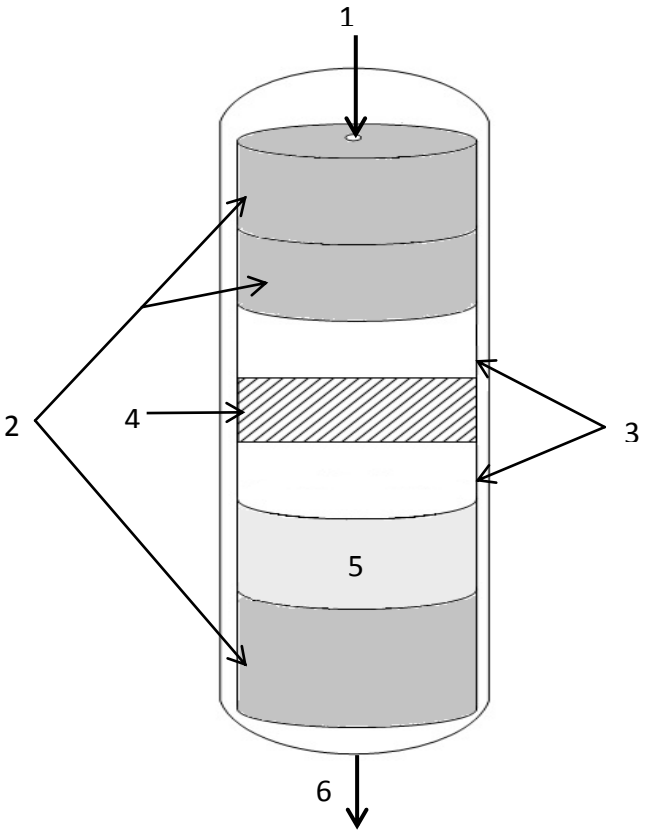

Figure 3.5 – Scheme of the centre section of the tubular reactor: 1) Reactant flow; 2) Stainless steel cylinders; 3) Quartz wool discs; 4) Fixed-bed; 5) Glass wool layer; 6) Product flow.

The catalyst was activated inside the reactor at 500 ℃ with 20 mL/min of nitrogen for 30 minutes, before each experiment. After that, the temperature has been set to the reaction temperature, 200 ℃.

Procedure

An accurate procedure has to be established to guarantee the reproducibilty of the experimental results. Before moving on to the catalytic tests themselves, preliminary tests were made. In these tests a procedure to guarantee that the injected reactant was entering in the system was made, and with each test we assured the resistance of the box section and reactor to the successive heating cycles.

The required amount of catalyst was charged in reactor, as shown in Figure 3.5. As shown in Figure 3.3, at first, it is needed to purge the line between the bottle and the inlet of the installation, opening valve (V1). After that we have to perform the catalyst activation. The schematic is represented in Appendix C – Different modes of the installation operation: Figure 8.6. Only the valves V3 (nitrogen flow), V7, V8 and V11 were opened. The activation conditions were described previously.

The next step is to fill the syringe pump with butene, which should be done to ensure the liquid state of butene. Before the syringe pump the 1-butene went through, an helical tube inside an ice bath before, to ensured once again the liquid state of butene. After that, the filling of syringe started at 2 mL/min; by setting this small rate we ensure that the liquid butene gradually enters the vessel.

In the preliminary tests, only the valve V1 (Figure 8.5) was opened. After completely filled the line, the valve was closed and the heating of the lines started. Then, the system was set to the reaction temperature controlled by 'Oligomerizacao_Reactor.exe' program. It is important that the temperature of lines and box section is well set, to guarantee that the reaction products are in the gas phase. Then, the system was put to the desired pressure, with nitrogen flow (V3, V6 and V9 open, and the remaining valves closed). After adjusting the pressure to 30 bar, all the conditions are set.

To perform the reaction, we have to set the nitrogen and butene flows, which were calculated from mass balance, based on the variables: catalyst mass (W), density of butene (ρ, calculated in section 4.2), molar masses (M_w of N_2 and butene) and reaction conditions (temperature and pressure). To start the reaction, valves V2, V3, V6, V9, V10 have to be opened and the remaining (V1, V4, V5, V7, V8, V11) closed. Then, with the installation appropriately prepared, the butene flow was started. The reactant mixed with N_2 travels through the installation and reacts in contact with the catalyst at the reaction temperature, and reaction products were collected in the cold trap while the gas phase is collected in loops in the GC at fixed times. This time can be fixed, normally distributed during the reaction. It should be guaranteed that the valve on GC is on the inject mode to fill the lopps. So, the gas products were analysed on-line and the liquid products identification was made separately in GC.

Finally, all the conditions to start the reaction were set and the injection of the butene and the nitrogen flow were started the collection of the samples and the loop loading can be started.

The experiments in this work were done at high pressure (30 bar) and at 200 ℃. During these experiments, the pressure tends to vary, so the manual BPR needs to be adjusted, to increase or decrease the pressure, depending on the system variations. Thus, it guarantees that the pressure remains stable along the assays. The effluent gas was periodically analyzed by gas chromatography equipment, that will be explained next. After the reactions a 20 mL/min flow of N_2 was used during 15 min to remove the remaining products inside the reactor and tubing.

3.5 GC Analysis

The characterization of oligomer products was done using Fast Gas-Chromatography – GC/FID. This equipment provides separation, qualitative and quantitative analysis for volatile, thermally stable compounds in a broad range of mixtures, from the simplest, as purity tests of individual compounds, to the most complex, such as petrochemical assays of samples comprising hundreds of individual components[90].

GC Characterization

The gas chromatograph (Dani, Italy) was equipped with a VB-1 capillary non-polar column with normal paraffins as reference. The separation column has a 60 meters length, 0.25 milimeters diameter and 1.5 µm film thickness and the temperature program varies between 40 and 330ªC. Helium was used as carrier gas. Two valves were placed in the lateral side of GC to allow gas storage for analysis or gas venting to purge. The gas chromatograph equipment was equipped with a flame ionization detector (FID), comprising with hydrogen and air as flammable gases. The GC is also equipped with a switch valve with eleven loops 500 µl each.

The more volatile products were analyzed on-line by after the trap line that is connected to the loops through the valve position load. Loop function can be seen in
Appendix E - Loop function(Figure 8.7 and Figure 8.8) as an example of the valves mode function, load and inject modes, respectively. The first valve position (Load) receives the stream from the trap and can send it either to the 11 positions valve or to the vent. The 11 position valve is used to store samples of the effluent stream at different times. The GC container were valves inject and load (Figure 3.2 - 15) needs to be at 200 ℃ temperature to avoid the gases to condense.

The loop acquisition was programmed at fixed times and distributed along the twelve loops during reaction. The liquid diesel from the trap was analyzed further by direct injection (0.5 µl) using a GC syringe and whithout dilution into the column in the septum.

Two distinct GC methods were carried out to analyze the gas and the liquid after the reaction. To analyze the gas phase, a program with temperature range from 40 up to 230 ℃ at 4℃/min, with a split ratio of 1/120, was used. For the liquid phase, a program with temperature range from 40 up to 300 ℃ at 20 ℃/min, with a split ratio of 1/80 was used.

Calibration

In order to analyze the products, a calibration of the Fast GC was needed. Using a solvent (toluene) into the ASTM D2887 Quantitative Calibration Mix has been used (200 µL from mixture for 2 mL of solvent). After turning the valve to load, the injection was performed the injection (1 µL of solution) with a syringe into the GC, and then, the method for the liquid analysis started. The peaks obtained are show in Figure 3.6.

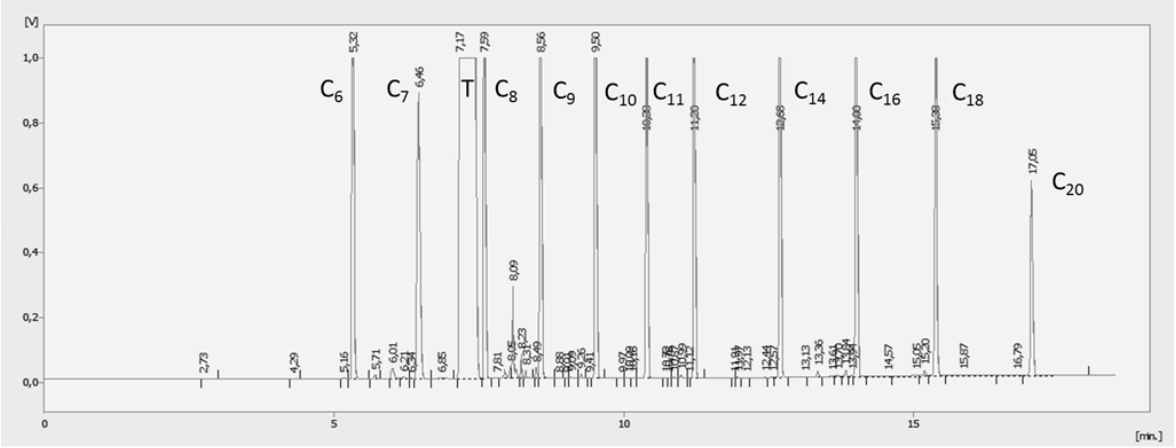

Figure 3.6 - The gas chromatogram of calibration mixture with the solvent (T=Toluene).

According to the characterization of the mixture, the present result obtained varies from C_6 to more than C_{20}. Therefore, the peaks can be characterized by output order, according to the mixture compound, as: hexane (C_6), heptane (C_7), toluene (solvent - T), octane (C_8), nonane (C_9), decane (C_{10}), undecane (C_{11}), dodecane (C_{12}), tetradecane (C_{14}), hexadecane (C_{16}), octadecane (C_{18}) and eicosane (C_{20}), as stated in the previous Figure 3.6.

The desirable range to obtain in these experiments is C_{10}-C_{20}. This is within the range of the calibration mixture.

Complementary tests

Besides the calibration described earlier, complementary tests have been made to samples provided by GALP refinery. The main objective of this procedure was to observe the detection of pure compounds and their mixtures by GC.

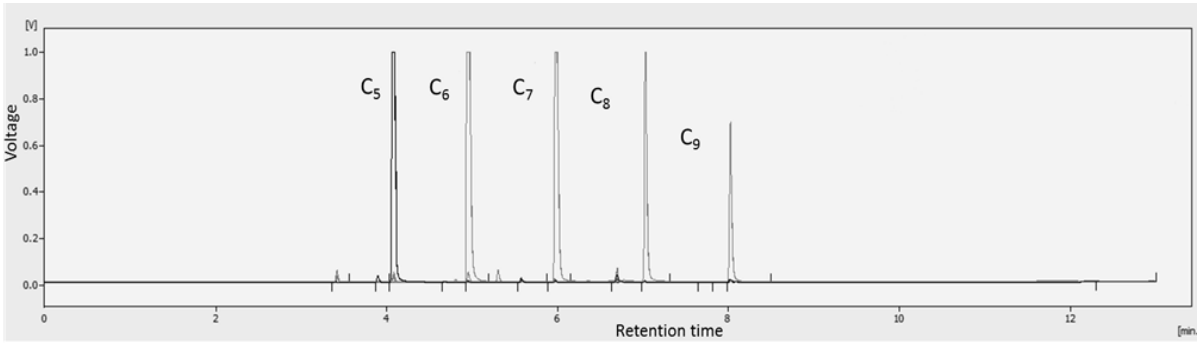

Figure 3.7 - The gas chromatogram from a mixture with pure compounds provided by GALP.

As noted in Figure 3.7, all the compounds came out in the expected order. According to the mixtures, the peaks match as pentane, hexane, heptane, octane and nonane. The compounds peaks came out in order of boiling point, as expected, thus the equipment responds well to the requirements of the experiments to perform.

All the results were obtained using the same split ratio (1:60) to provide equal conditions of analysis.

4. Modeling

4.1 Introduction

The main focus of this chapter is the calculation of 1-butene density, and the development of the mathematical model to predict the oligomerization results. The 1-butene density was calculated from the Peng-Robinson equation of state.

4.2 Density of 1-butene (PREOS)

The Peng-Robinson equation of state was used to calculate the molar volume pure 1-butene as function of pressure and temperature. This equation expresses fluid properties in terms of the critical properties and acentric factor of the species involved.

$$\rho = \frac{M}{V_m} \tag{4.1}$$

$$P = \frac{RT}{V_m - b} - \frac{a.\alpha}{V_m^2 - 2bV_m - b^2} \tag{4.2}$$

$$a = \frac{0.45724\, R^2 T_c^2}{P_c} \tag{4.3}$$

$$b = \frac{0.07780\, R\, T_c}{P_c} \tag{4.4}$$

$$\alpha = [1 + (0.37464 + 1.54226\omega - 0.26992\omega^2)(1 - T_r^{0.5})]^2 \tag{4.5}$$

where, P is pressure, V_m is molar volume, T_c is critical pressure, P_c is critical pressure and ω the acentric factor. The results are shown in Table 4.1, at T and P (0℃ and 30 bar), used to pump 1-butene.

Table 4.1 - Butene critical properties and parameters of Peng-Robinson equation of state (P=2.8 bar, T=0°C).

1-Butene Properties (Pure Fluid)								
T_c (K)	P_c (MPa)	ω	R (cm^3 MPa/mol K)	T_r	a (MPa $cm^6/g.mol^2$)	b (cm^3/g.mol)	V_m (cm^3/mol)	ρ (g/cm^3)
145,85	4,020	0,187	8,314	0,7106	1755815	67,51	85,60	0,655

Now that we know the density of the butene, we can calculate the butene flow for each experiment process and the respective injected mass of reactant (m_{butene}= 13 g).

4.3 Math Model

Concerning oligomerization modeling, several models were studied over the last years[6, 20, 48, 91]. After some research, the model that best suited this work was the one proposed by Alberty[92]. Several steps were made in order to apply this model to characterize this system. This aproaches focus on the extrapolation of standard chemical thermodynamic properties of alkene isomer groups to higher carbon numbers[93] based on the data of standard chemical properties of alkene isomer groups, available in the literature and presented by Alberty and Catherine[94]. This model is very versatile, allowing us to study the influence of several variables like pressure, temperature, type of reactant, feed composition on the kinetics[92] and thermodynamics[93] of the oligomerization.

Thermodynamics of Alkene Oligomerization

In order to formulate a model, thermodynamic data of all intervening components in the reaction are needed. As shown in Table 4.2, the equilibrium computations become impractical with the inclusion of all isomers involved above C_7 or C_8. In any case, the thermodynamic properties for all olefin isomers are only known up to hexene with additional data on linear 1-olefins available up to C_{20}.

Table 4.2 - Complexity of olefin mixture due isomerization.

Carbon Number	Olefin Isomers number
3	1
6	18
10	895
15	185 310
20	46 244 031
25	12 704 949 506

So, this computations can be greatly simplified by the fact that when a group of isomers are in equilibrium with each other, they can be treated as a single compound in calculating their equilibrium with other compounds. Calculating the lumped free energy of the isomer group exactly still requires knowledge of the individual isomer free energy, which are currently known only up to six carbons atoms.

A rigorous thermodynamic analysis of oligomerization reactions is difficult since there are relatively few data available on the thermodynamic properties of isomers and alkenes with molecular weight greater than that of hexenes[5,95]. This has required the use of group thermodynamic properties[96]. By this approach, alkene distributions were computed using free-energy data for the n-1-alkenes and also using the equilibrated isomer group data. The basis behind this assumption is that the relative distribution of isomers in a carbon number group depends only on temperature and not on the overall composition of the system. The standard Gibbs free energy of the isomer group is then given by the summation over all individual isomers i and a free energy of mixing term:

$$\Delta G_{fI}^{o} = \sum_{i} r_i \Delta G_{fi} + RT = -RTln \sum_{i} e^{-\Delta G_{fi}/RT} \qquad \textbf{4.6}$$

where r is the fraction of isomer I in the group and ΔG_{fi} is the standard Gibbs free energy of formation of isomer I. Because of the difficulty of this approach, that rises from the knowing the thermodynamic data on all individual isomers, Alberty[94] developed an approximation method to estimate the group thermodynamic properties by assuming a linear extrapolation form:

$$\Delta G_{fi}^{o} = A + Bn \qquad \textbf{4.7}$$

where A and B are constants at given temperature and n is the carbon number of the isomer group. The constants are calculated from the known properties of alkenes. The enthalpy of formation of an isomer group is obtained by an analogous expression:

$$\Delta H_{fi}^{o} = A_h + B_n n \qquad \textbf{4.8}$$

Hence, the standard Gibbs free energy formation for an isomer group at any temperature range can be approximated by

$$\Delta G_{fi}^{o}(T) = \Delta G_{fi}^{o}(T_0) + \int_{T_0}^{T} \frac{\Delta H_{fi}^{o}}{RT^2} dT \qquad \textbf{4.9}$$

These should give reasonable estimate if they are not extrapolated too far[97].

In this case this approach is acceptable because the product range obtained in this work, (diesel range - up to C_{20}), fits on this approximation.

The data calculated took into account the Gibbs free energy of isomers up to C_6[95], and extrapolated by linear estimation for compounds higher than C_6 that is available[5, 94]. The equilibrium of alkene oligomerization can be predicted with this isomer groups aproximation which allows to predict the equilibrium distributions and refer each component as a group of isomers. With the existing data, it is possible to calculate the equilibrium constants for each step through equation 4.10.

$$K_P = \exp\left(-\frac{\Delta G_{fI}^{i+j} - \Delta G_{fI}^{i} - \Delta G_{fI}^{j}}{RT}\right) \qquad \textbf{4.10}$$

where K_P is the equilibrium constant, ΔG_{fI}^{i+j} the product Gibbs free energy of formation, ΔG_{fI}^{i} and ΔG_{fI}^{j} for the reactants i and j Gibbs free energy of formation .

However, many isomers are excluded from the pores of H-ZSM-5 catalyst by steric hindrance. Thus, for our system we need to estimate properties of groups containing only those isomers for which the catalytically active pores of the zeolite are accessible. Another consideration is the departure of the system from ideal gas behavior[5].

Kinetics of Alkene Oligomerization

In order to develop a kinetic model for the oligomerization of light alkenes it may be assumed that the isomers of a particular carbon number are at equilibrium, as explained before. This enables the product spectrum to be split into groups or lumps representing each carbon number[98]. Although in the development of such a model it is assumed that double bond and skeletal isomerization are significantly faster than oligomerization or cracking reactions, it has recently been shown that at low conversions only the double bond isomers and the skeletal isomers are at equilibrium[99]. On the basis of the continuous product spectrum obtained at high conversions, it can also be assumed that the reaction rates undergo a gradual change from one carbon number to another.

Alberty [92] developed a kinetic model to describe the oligomerization of alkenes on zeolites, in order to obtain gasoline or diesel using H-ZSM-5 catalyst in the temperature range of 177-377°C. Knowing the necessary alkenes thermodynamic properties, described above, are describes now the reactions rate constants. Butene oligomerizes to C_8, C_{12}, C_{16}, C_{18}, etc., and these products can crack and polymerize to an almost continuous distribution of isomer groups at an equilibrium

that depends on temperature, pressure and catalyst selectivity. The isomerization reaction occurs more rapidly on H-ZSM-5 than polymerization and cracking reactions. Thus the study of kinetics of alkene polymerization provides an opportunity to learn about the rates of cracking and oligomerization reactions of isomers groups.

The reaction can be described by the mechanism represented in the Figure 4.1.

$2C_4H_8 \rightleftharpoons C_8H_{16}$	**(a)**	$C_8H_{16} \rightleftharpoons 2C_4H_8$	**(b)**
$C_4H_8 + C_8H_{16} \rightleftharpoons C_{12}H_{24}$		$C_{12}H_{24} \rightleftharpoons C_8H_{16} + C_4H_8$	
$2C_8H_{16} \rightleftharpoons C_{16}H_{32}$		$C_{16}H_{32} \rightleftharpoons C_8H_{16} + C_8H_{16}$	
...		...	

Figure 4.1 - Several possible steps in the oligomerization of butene (a) and cracking reactions (b).

In the absence of data on the individual rate constants, calculations have been made on the basis of either one of two assumptions: (1) the bimolecular rate constants can all be assumed to be equal, and the cracking constant for each step is calculated using the Gibbs energies of formation of the isomer groups involved in that step, or (2) the cracking rate constants are assumed to be equal, and the bimolecular rate constant for each step is calculated from the Gibbs energies of formation. In the absence of detailed data, both assumptions are plausible. In support of assumption (1) the bimolecular reactions come together to form a single alkene molecule. In support of assumption (2) the cracking reactions are all very similar, each involving breaking an alkene molecule into two alkene molecules. Therefore, reaction constants calculations have been made here with each assumption. Since k_f, the rate constants for forward reactions (bimolecular), and k_b are unknown, the assumptions were made using the effective rate constants, k'_f and k'_b, given by one of the assumptions:

Assumption (1)
$$k'_f = 1 \rightarrow k'_b = \frac{P^0 K_P}{P} . k'_f \qquad \textbf{4.11}$$

Assumption (2)
$$k'_f = K_P \rightarrow k'_b = \frac{P^0}{P} \qquad \textbf{4.12}$$

where k'_b is the effective rate constant for the backward reaction and k'_f is the effective rate constant for the forward reaction.

Numerical integrations of rate equations for mechanism

The use of matrix notation simplifies both the theory and computer programming involved in the numerical integration of the differential equations corresponding with a mechanism of reaction. A mechanism involving N species A_i; (in this case isomer groups) and R the reaction steps are represented by:

$$0 = \sum_{i=1}^{N} v_{ij} A_i, \qquad j = 1, \dots, R. \tag{4.13}$$

The stoichiometric coefficients, v_{ij}, positive for products and negative for reactants. In calculating equilibrium compositions, all that is required is a set of independent reactions that can represent all possible chemical changes in the system. Of course, the number N of steps in the mechanism must be equal to or greater than the number of independent reactions R.

The calculation of the amounts $\mathbf{n_i}$ of the species involved in the mechanism as a function of time is given from the extent of reaction by:

$$\mathbf{n_i} = \mathbf{n_i^0} + \sum_{j=1}^{R} \boldsymbol{\upsilon_{ij}} \boldsymbol{\xi_j} \qquad i = 1, \dots, N. \tag{4.14}$$

This equation is readily converted to matrix form. The matrix $\boldsymbol{\upsilon}$ is referred to as the complete stoichiometric coefficient matrix by Smith and Missen[100] who use the symbol N for this matrix.

The basic kinetic equation for a mechanism is obtained by a material balance to the system:

$$\frac{d\mathbf{n}}{dt} = \boldsymbol{\upsilon} \frac{d\boldsymbol{\xi}}{dt} = \boldsymbol{\upsilon} \boldsymbol{r} \tag{4.15}$$

The matrixes $d\boldsymbol{\xi}/dt$ or $\boldsymbol{r}$ can be referred to as the conversion matrix or net rate matrix, following the IUPAC recommendation[101] that $d\xi_j/dt$ is the rate of conversion for a single reaction.

Oligomerization of a gas with a heterogeneous catalyst is most conveniently carried out at constant pressure using a flow system. The calculations presented here apply to an isothermal-isobaric process. The forms of the equations for the net rates r_j need to be derived for constant pressure and for the two assumptions stated earlier.

This approach can be interesting to apply in our system because, depending on the conditions used, we could predict the results obtained.

Numerical integrations of the set of 20 simultaneous rate equations represented by:

$$\frac{d\mathbf{n}}{d\tau} = \boldsymbol{\upsilon} r \qquad \textbf{4.16}$$

were carried out using the fourth order Runge-Kutta method [102] on MatLab. The species abundance matrix after a short time interval h is given by:

$$\mathbf{n}_{k+1} = \mathbf{n}_k + h\boldsymbol{\upsilon}\mathbf{r}' \qquad \textbf{4.17}$$

where the net rate matrix is evaluated with $\boldsymbol{r}'$.

The programs utilized the vector formulation of the Runge-Kutta method [103], in order to calculate the initial values of $n_2, \ldots n_{20}$. Then, for each step, the net rates r_j can be calculated for the next iteration. By combining the net rate with equation 4.11 it is obtained that:

$$r_1{}' = \frac{d\xi_1}{d\tau} = \frac{P^0}{Pk_b}\frac{d\xi_1}{dt} = \frac{K_P n_2^2}{\sum n_i} - \frac{P^0 n_4}{P} \qquad \textbf{4.18}$$

where

$$\tau = \left({}^{P}/_{P^0}\right) k_b t \qquad \textbf{4.19}$$

P is the system pressure, P^0 standard pressure (1 bar), t is the time, $d\xi_1/d\tau$ the rate of conversion, τ the dimensionless time, n_2 and n_4 the molar fractions of ethene and butene, for one particullary case. This will be expressed in terms of effective rate constants by equation 4.20.

$$r_1{}' = \frac{k_f' n_2^2}{\sum n_i} - k_b' n_4 \qquad \textbf{4.20}$$

where k_f' represents the effective rate constant for forward reactions and k_b' the backward reactions rate constants, which will be calculated for either assumptions.

Using this approach, we could predict the behavior of alkene oligomerization in terms of composition along reaction time. This model has been developed by Alberty [92] up to C_{13} products and was extrapolated for products up to C_{20}. This required 81 possible reactions steps in this process, instead of the original 30.

Regarding the operating conditions, this model also allows to vary the system temperature and pressure. This gives plenty information about the behavior of the oligomerization reaction, by setting the reaction time (or catalyst contact time), the reactant to be used to feed the system, and the temperature and pressure of operation. Therefore, with this data set it will be possible to analyze the system response on the defined conditions.

5. Results and Discussion

5.1 Introduction

In this section the characterization of the H-ZSM-5 (CBV 3024E), its physico-chemical characteristics will be discussed. Also, the experimental and modeling results are shown and analyzed.

5.2 H-ZSM-5 (CBV 3024E) Characterization

Physico-chemical characteristics of H-ZSM-5 zeolite

The difference between this value and the value provided by the manufacturer (Si/Al = 15) can be due to the differences in the analytical methods. The chemical composition of the calcined material presented a Si/Al of 19. The catalyst is in ammonium form with surface area of 400 m^2/g and Na_2O of 0.05% weight[83].

Crystal sizes and morphology were analyzed from SEM pictures shown in Figure 5.1. As it is shown the catalyst has the same crystal size and morphology, before and after calcination.

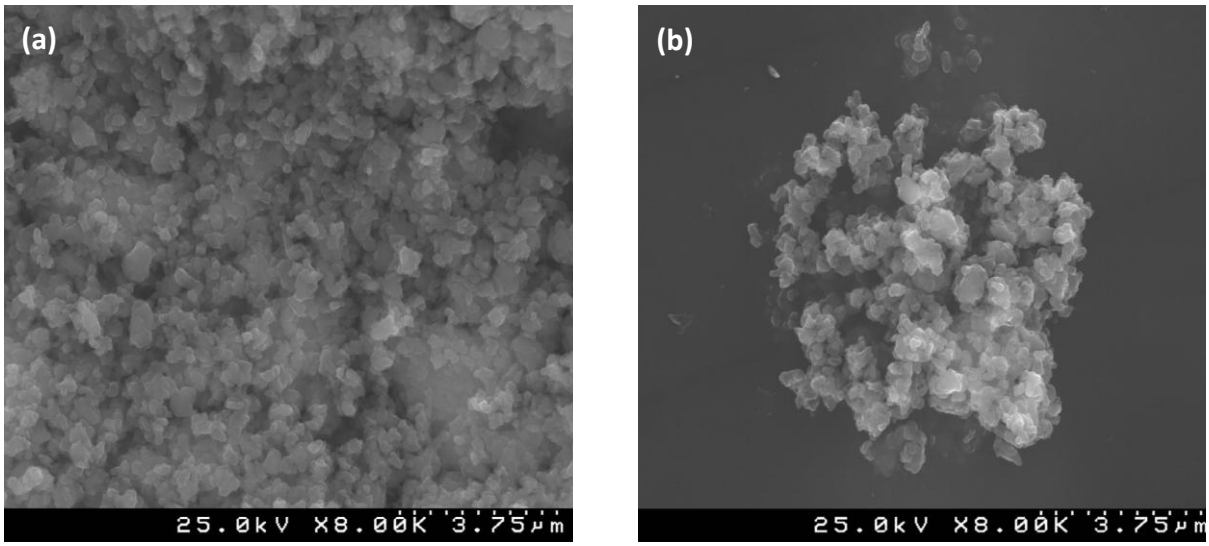

Figure 5.1 - SEM of 15H H-ZSM-5 CBV 3024E catalyst before (a) and after calcination (b).

Moreover, all base lines were straight, implying that no amorphous fractions were present and the materials are highly crystalline. Comparing the peak intensities of XRD confirmed that the catalyst used (CBV 3024E) matches the H-ZSM-5 reference, as show in Figure 5.2.

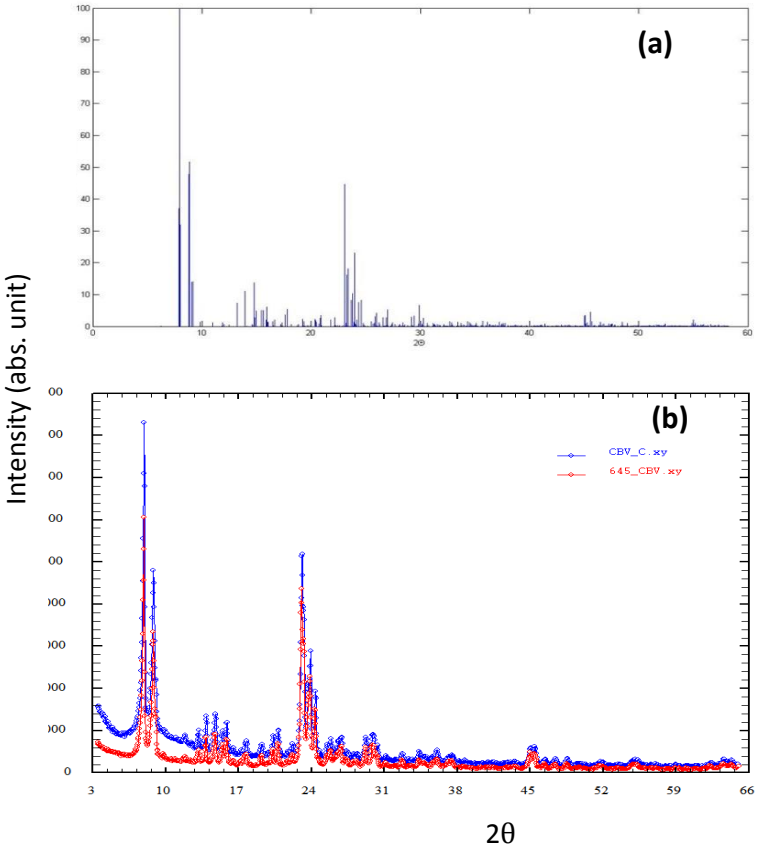

Figure 5.2 - XRD results from the H-ZSM-5 (a) reference and (b) the CBV 3024E used[83].

5.3 Experimental Results

A significant part of this thesis was spent in the preparation of the installation for future experimental works. One method to acquire the products into the trap has been devised. The recoil consists in a cup, designed and made to adjust into the trap as shown in Figure 5.3.

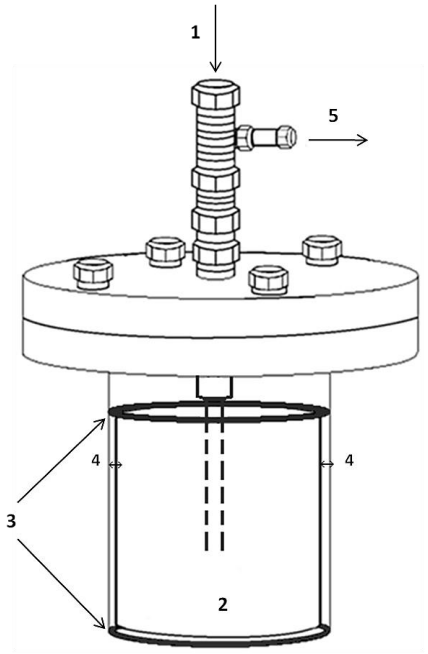

Figure 5.3 - The trap with the cup scheme: 1) Products Flow; 2) Cup; 3) O-rings; 4) Gap between the trap and the cup; 5) Gas Product flow.

The product stream enters into the trap (1) and is collected in the cup where one o-ring between glass and steel avoids loss of product; another o-ring in the base protects the glass (4). Other o-ring also exists bettween the external stainless steel cup and its cover to seal the entire trap. Since the trap is cooled (ice bath), the more volatile products (C_5-C_6 or even dimers at the most) may be in vapour-liquid equilibrium some of the vapour goes up to (5).

Few works at high pressure in light olefin oligomerization processes have been reported so far, thus, the option to use high pressure system was choosed. Several repetitions have been made, in order to obtain reprodubility. Operating conditions and obtained data are shown in Table 5.1. The catalyst pre-treament has been equal in every experiments, with 500 ℃, 30 min, 20 mL/min N_2. The Line In, Line Out, Box section, BPR, Trap-GC, temperatures were 180, 200, 200, 200, 120 ℃ respectively.

Table 5.1 – Experimental conditions and results of the butene oligomerization.

Butene M_W (g/mol)					56,11			Butene Molar Volume (cm^3/mol)			85,60		
Nitrogen M_W (g/mol)					28,01			Butene ρ_o (g/cm^3)			0,655		
Syringe Volume (mL)					20,00			Mass of liquid injected (g)			13,11		
Experiment	Catalyst weight (g)	Reaction Pressure (bar)	N_2 Flow Rate (cm^3/min)	Reaction Temperature (°C)	Butene Flow Rate (cm^3/min)	Reaction Time (min)	Butene mass flow rate (g/min)	Feed Butene Fraction (wt. %)	WHSV (h^{-1})	Product Liquid weight (g)	Reactant liquid weight (g)	Yield (%)	Notes
1	0,505	30	4,66	200	0,122	164	0,080	7	9,50	0	13	0,0	Valve number 1 wasn't closed
2	0,503	30	4,64	200	0,122	164	0,080	7	9,54	0	13	0,0	No product formation
3	0,513	30	4,79	200	0,087	230	0,057	10	6,67	2,368	13	18,1	Diesel Products
4	0,503	30	4,70	200	0,0852	235	0,056	10	6,66	1,052	13	8,0	Diesel Products
5	0,503	30	4,70	200	0,037	541	0,024	20	2,89	-	-	-	No product formation

The only one thing that varied was the gas phase loop acquisition, that is displayed in appendix section on Table 8.2.

The first and the second experiment were preliminary tests. There was no product formation, but have served to improve the procedure. So, it only makes sense to consider the experiments in grey and the liquid formation detected. In the third experiment the yield was 18.1 % and in the fourth was 8 % which has been very low.

The products were analyzed in the gas chromatograph. The gas phase was analyzed along reaction using the eleven loops available in order to detect the steady state and the volatile products formed. The loops acquisition were set at intervals of 30 min for each loop, until steady state was reached. It can be seen in Figure 5.4 that the steady state formed essentially dimers as products. A second experiment the same conditions has been made and the results were similar.

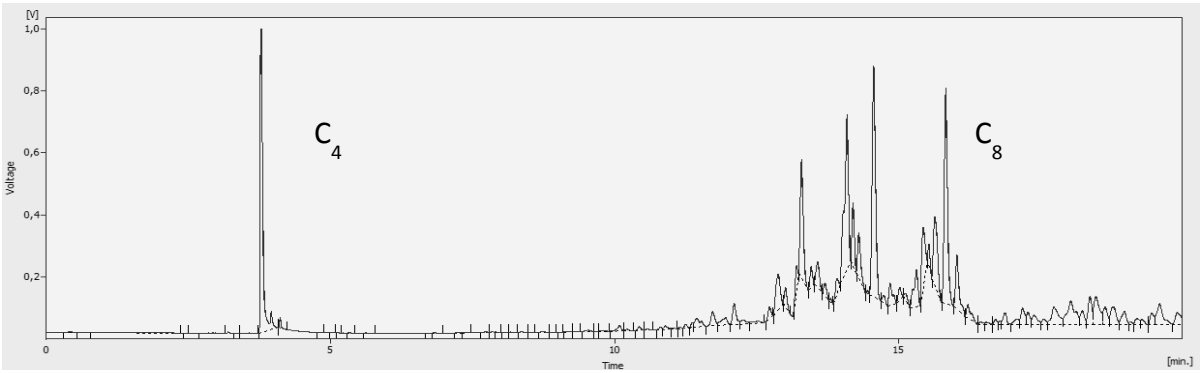

Figure 5.4 - Gas phase chromatogram (steady-state) of gas products of run number three of Table 5.1.

Afterwards, the liquid phase was analyzed by injection using a syringe with 0.5 µL. The chromatogram obtained is shown in Figure 5.5.

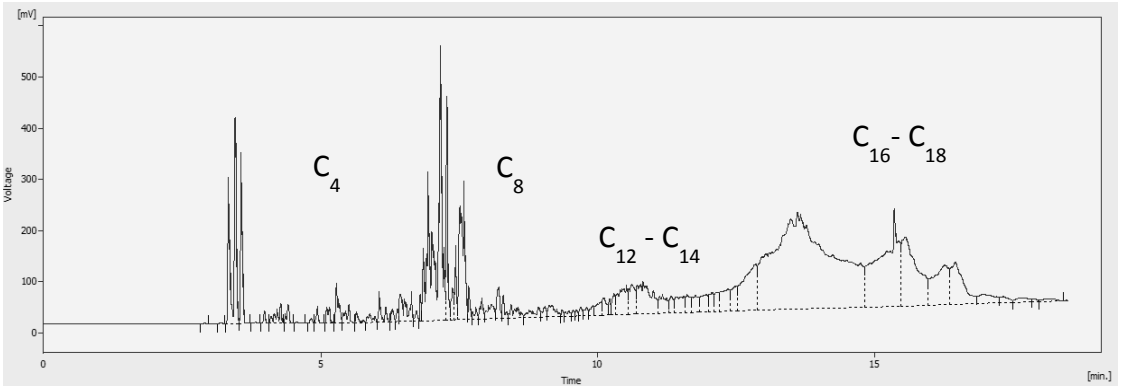

Figure 5.5 - Gas phase chromatogram of the liquid product of run number three of Table 5.1.

It is shown that the liquid phase product contains dimers (C_8), trimers (C_{12}) and tetramers (C_{16}). This range of products revealed that the oligomerization process succeded, with products in C_{16}-C_{18} range. By visual analysis of the area of the peaks, it can be stated that the quantity of C_{10}-C_{18} is higher than the remaining compounds which matches the diesel range.

In Figure 5.6 we present the results from the literature by Rodriguez et al.[104]. The diesel reference is shown above, and three experiments gave resulted in the chromatograms P1, P2 and P3. It was used 1-hexene with different amounts of nitrogen and sulfur compounds (P1 and P2) and FCC naphta (C_3-C_6 compounds - P3) as feed. The three products showed the type of tendency that oligomerization reactions should have. Compared with Figure 5.6, our results exhibit the same peaks trend.

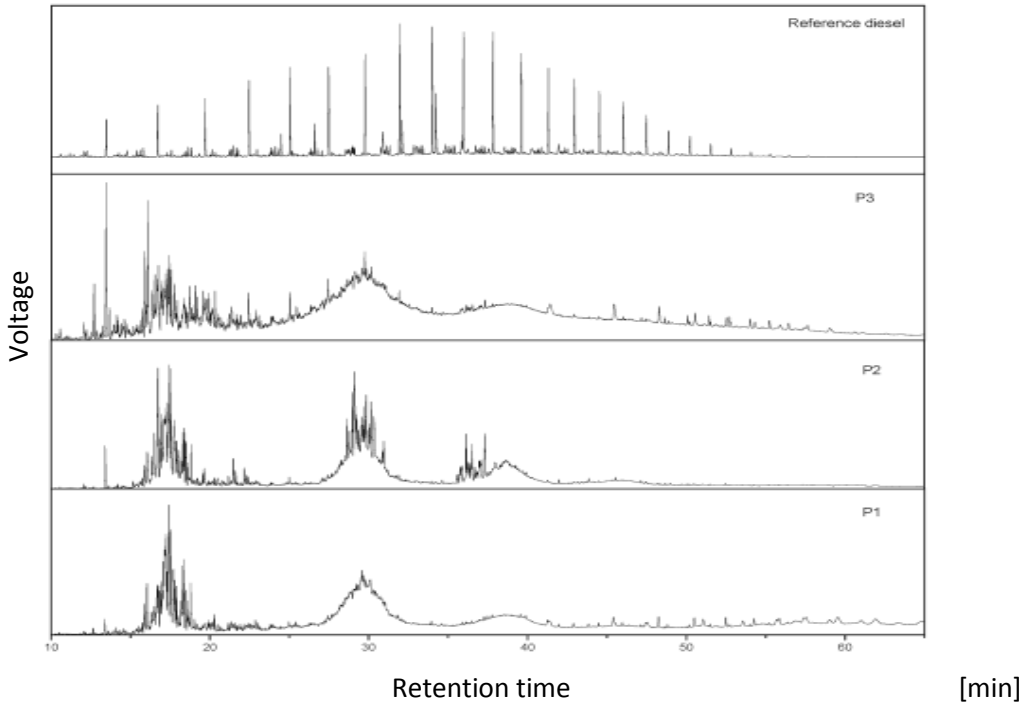

Figure 5.6 - MS spectra for oligomerization mixtures and reference diesel [104].

Another study with 2-butene oligomerization to heavy olefins over H-ZSM-5 zeolite has been made by Liu et al.[43]. The work is very similar to the one performed in this thesis and the gas chromatograms of products obtained by different reaction temperature are shown in Figure 5.7. These chromatograms trends also match those in Figure 5.5.

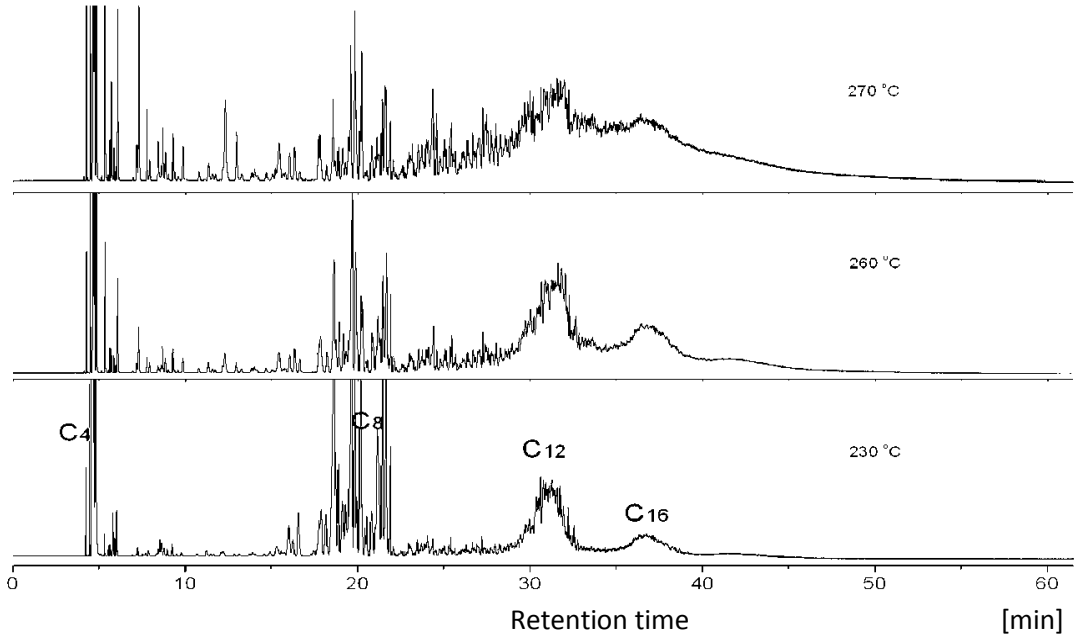

Figure 5.7 - Gas chromatograms of products for the oligomerization of 2-butene over H-ZSM-5 at varying reaction temperatures[43].

It can also be noticed that the usual approach in this kind of work lies on the fact that the chromatograms analysis uses compounds combination, since it is impossible to treat all individual contributions of isomers.

After the analysis of the obtained peaks, the chromatogram trends and their positions are consistent with the expected.

The experiments at higher pressure allowed to obtain the compounds in the required range, unlike some authors[18, 42, 105]. The lower yield can be explained by trap malfunction, possible product accumulation inside the tubing system or, inflow reactant conditions.

Between experiments, simple nitrogen flow is not enough to wash the tubing system. Hence, an additional cleaning with hexane was performed in order to collect the heavier hydrocarbons. In this way, the installation get ready for new runs.

5.4 Modeling results

As stated earlier, the oligomerization reaction depends on several conditions, such as temperature, pressure, catalyst type or reaction time (or space time). Applying the model presented Chapter 4, one may predict the reaction behaviour for the operating conditions chosen.

Using assumption (1) and 1-butene (pure feed) and varying the dimensionless time, τ, the light olefin conversion and its products formation are shown in Figure 5.8.

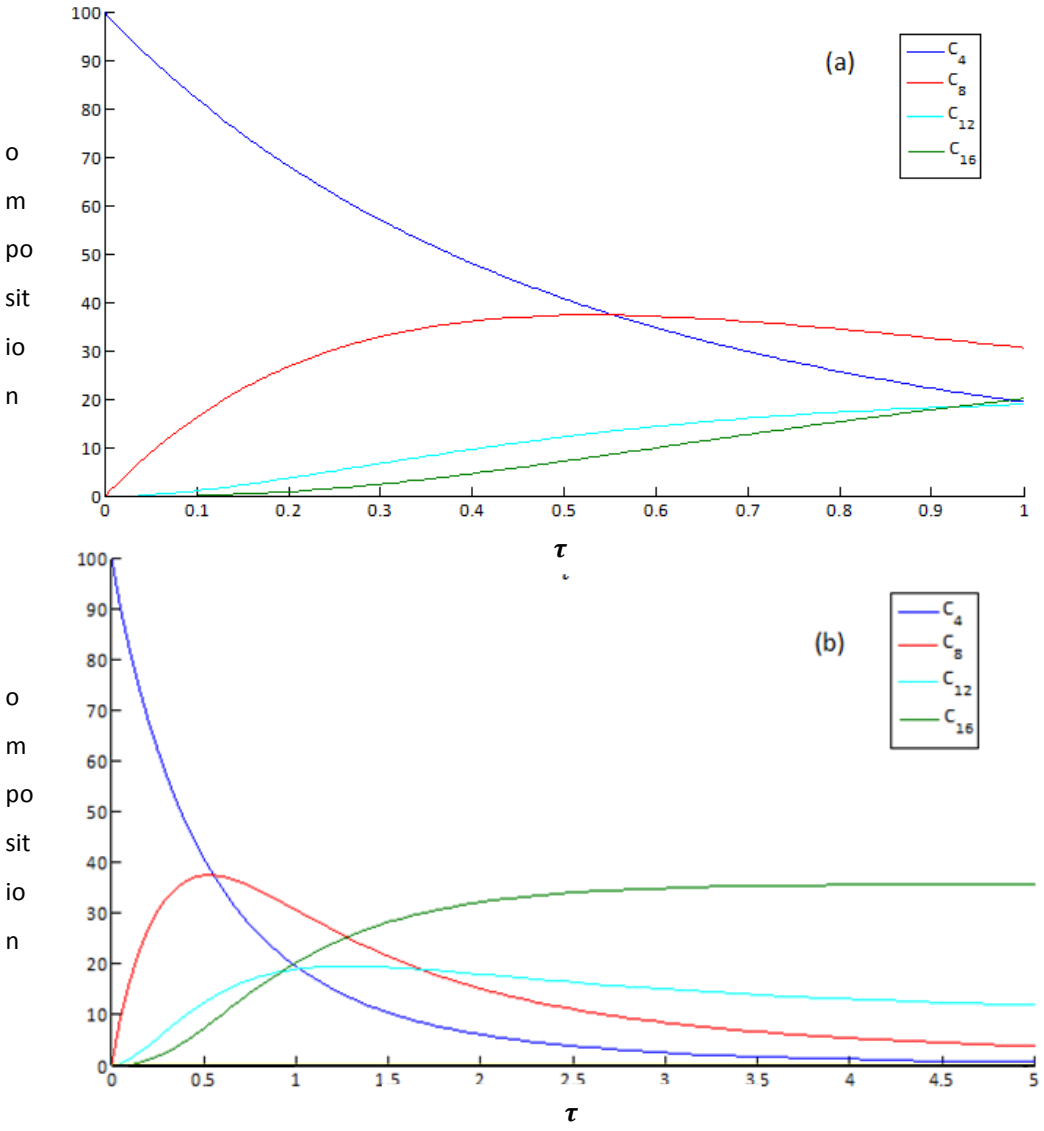

Figure 5.8 - Weight percentages of isomer groups obtained from the oligomerization of pure butene as function of time at 200℃ and 30 bar for (a) τ<1 and (b) τ<5, with pure butene as feed.

As depicted in Figure 5.8. a, for short times (τ<1) the products formed were mostly dimers (C_8) and trimers (C_{12}) range. This means that lower contact times between the reactant and the catalyst results in lower conversion and the formation of small hydrocarbons. At higher τ, more compounds diesel range are formed. This fact is supported by Figure 5.8 b. With the increase of contact time, it is observed as expected that trimers and tetramers are the product that will be produced in higher amount, over the remaining the oligomers. The product range is up to diesel range (C_{16}) and the conversion of the reactant is almost 100 % at τ=5.

Obviously the system tends to an equilibrium, when $\tau \rightarrow \infty$. This means that time is extremely important in the process. Besides that, two other variables are studied and play an important role on the olefin equilibrium: the temperature and pressure.

As stated in the first chapters, the alkene oligomerization is highly exothermic reaction. By this fact, increasing the temperature does not favour the equilibrium conversion, since it causes the decline of the average carbon number, cracking. This fact is supported by this model and from literature[5, 106]. This is shown in Figure 5.9 and Figure 5.10, for atmospheric pressure and for higher pressure (30 bar), respectively.

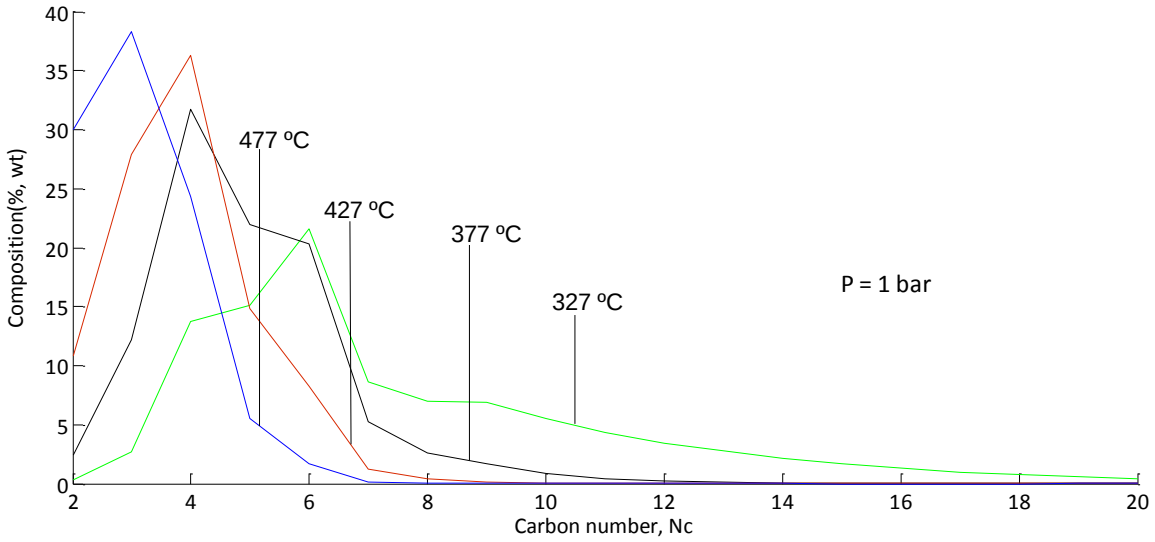

Figure 5.9 - Effect of temperature on olefin distribution at equilibrium (τ=50) at 1 bar.

The model implemented in this work shows the temperature effect, in the 327-477 ºC range, at atmospheric pressure with success. As illustrated in Figure 5.9, by fixing the pressure and varying the temperaure, the olefin distibutions at equilibrium is predicted. As specified before, the temperature does not favour large molecules, since the cracking reactions are

favored, the higher hydrocarbons compounds in the mixture decreases. It can be concluded that cracking reactions become relevant, leading to higher amount of lighter olefins at equilibrium.

In terms of pressure, similar calculations have been performed in order to evaluate even better the results obtained in the Figure 5.9. By increasing the pressure to 30 bar, the model allows us to characterized the system behavior at 377-477 °C. These results can be compared to the ones in Figure 5.9 at 1 atm.

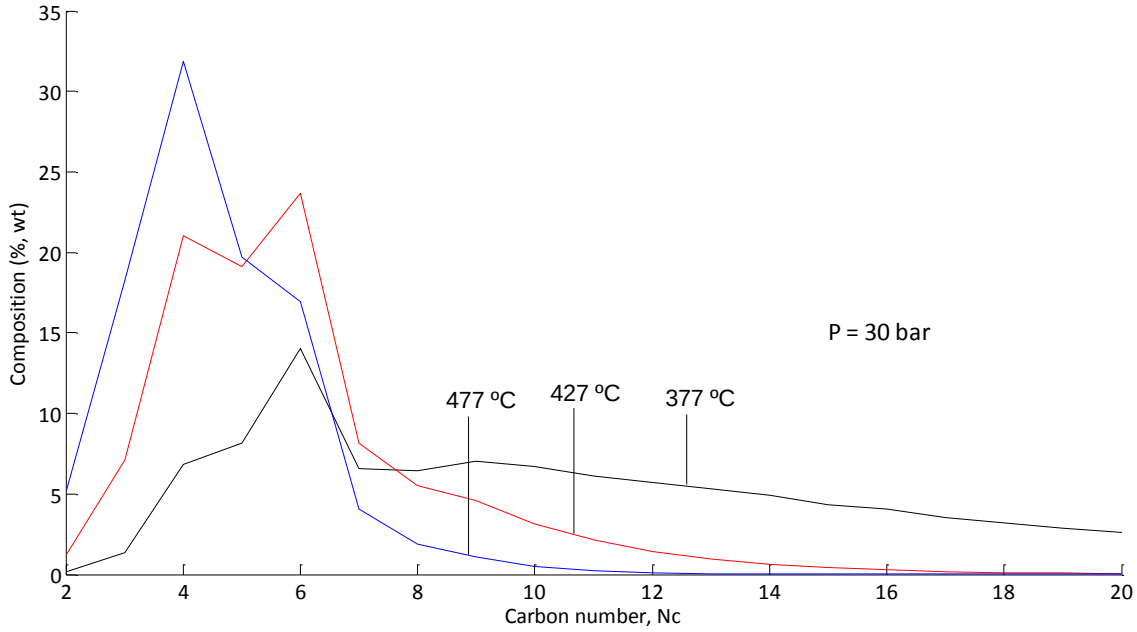

Figure 5.10 - Effect of temperature on olefin distribution at equilibrium (τ=50) at 30 bar .

By increasing pressure from 1 to 30 bar, two considerations can be taken. The first one is that the same trends for temperature are observed in both figures, i.e., the increase of temperature does not favour heavier hydrocarbon at equilibrium. The second one is that higher pressure promotes higher amount of large hydrocarbons at equilibrium. For instance, at the same temperature, if individual isotherms of Figure 5.9 and Figure 5.10 are compared, those for 30 bar lie above the atmospheric ones.

After analyzing the temperature effect at constant pressure, the effect of pressure on the olefin equilibrium can also be a matter of study. This effect was previously observed and now it is clearly shown in Figure 5.11, at fixed temperature, for several isobarics.

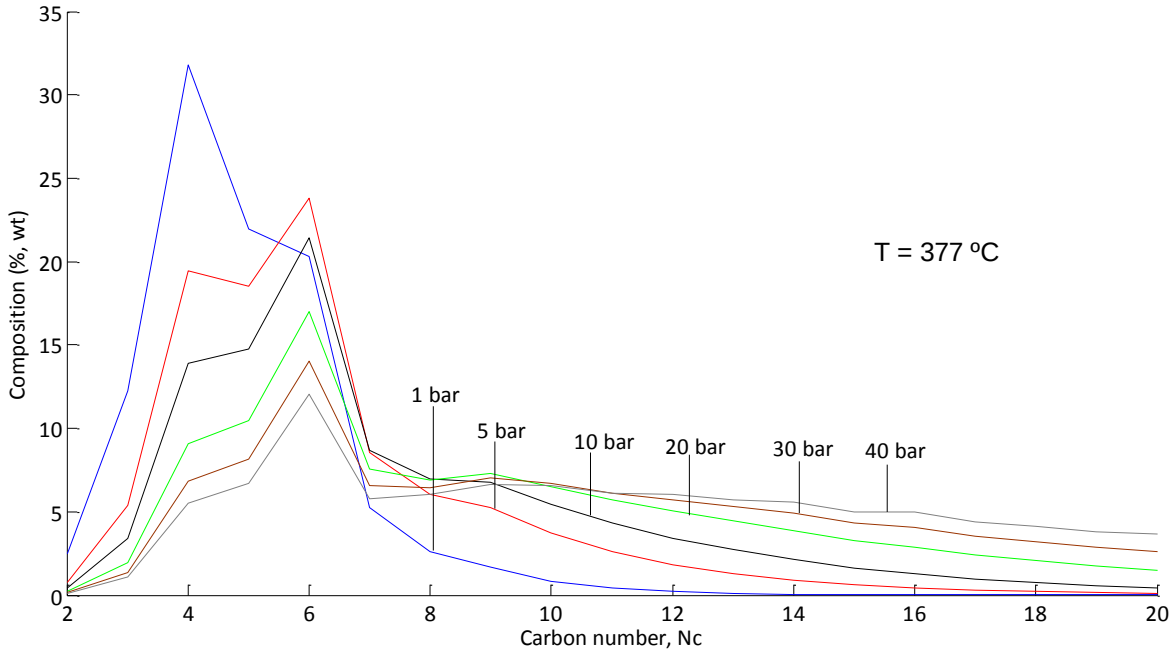

Figure 5.11 - Effect of pressure on olefin distribution at equilibrium (τ=50) at 377 ℃.

As illustrated in Figure 5.11 (at 377 °C), the increase of pressure reflects on higher amount of compounds with higher carbon number. However, this increase at much higher pressure becomes less significant.

This can be explained by the Chatelier's principle. By increasing the system pressure, the system reacts to counter that effect. So, in this case, increasing the pressure, results in the formation of the smallest possible number of molecules, i.e. favors oligomerization of higher carbon number: for example, two molecules of C_4 form one molecule of C_8.This behavior, along with the H-ZSM-5 selectivity that tends to generate more linear compounds, as specified before, allows the obtention high quality distillate products.

6. Conclusions and Final Remarks

With the objetive to ensure diesel quality and overcome its increasing demand, in comparison with gasoline, oligomerization processes become an important matter of subject. In this sense, an installation was prepared to study the operating conditions with 1-butene as feed. The system pressure is a very important variable in this exothermic reaction, and there are few studies about its effect. When increased, the system tends to form compounds with higher carbon numbers. This fact combined with the H-ZSM-5 shape-selective effect, tends to generate higher linear carbon number molecules, ie, high quality diesel.

During the set-up of the oligomerization unit, various tests were necessary. Leak tests with several heating cycles were required, in order to ensure that the system was tight. The reactant used, 1-butene, is flammable and the system isolation is an extremely important factor to be taken into account, for safety reasons.

After the installation check-up, the catalyst activation and pre-treatment, several runs have been carried out at the same conditions. Only two experimental conditions formed the desired product. However, the yield wasn't very significant (18.1 % and 8 %). Nevertheless, the GC analyzis proved, in qualitative terms, that diesel has been formed.

The yield was not very significant (18.1 % and 8 %). However, the GC analysis proved that diesel has been formed. At this stage the main objective was the installation of the unit, the calibration of GC, and choice operationg conditions that ensure diesel production.

Concerning modeling, after a deep bibliographic search, the approaches were selected and implemented computationally in Matlab, in order to study the influence of temperature, pressure and reaction time upon oligomerization. By fixing the pressure and varying the temperature, the model showed that increasing temperature does not favour the formation of compounds with high carbon numbers. On the contrary, at constant temperature as pressure rises, compounds with higher carbon numbers are formed. This effect was expected because oligomerization is an exothermic reaction, so higher temperatures does not favor direct reaction. Moreover, it favours cracking reactions. Regarding pressure, its increase promotes the direct reactions, ie, the oligomerization. The study of pressure in this process is a matter that needs more research and this model is a good way to support it.

In summary, this thesis was an important step for the study and optimization of light olefins oligomerization. As has been discussed in the introduction, the implementation of alkenes oligomerization units is believed to be a very profitable way to produce diesel.

7. References

1. E. Kriván, G.M., J. Hancsók, *Investigation of the Oligomerization of Light Olefins on Ion Exchange Resin Catalyst.* Hungarian Journal of Industrial Chemistry Veszprém, 2010. **38 (1)**: p. 53-57.
2. Kaufmann, T.G.K., A.; Stuntz, G. F.; Kerby, M. C.; Ansell, L. L., *Catalysis science and technology for cleaner transportation fuels.* Catalysis Today, 2000. **62**(1): p. 77-90.
3. G. Bellussi, A.C., R. Millini, in *Zeolites and Catalysis*, A.C. J. Cejka, S. Zones (Eds.), Editor 2010, WILEY-VCH Verlag GmbH & Co. p. 449-491.
4. Group, C.R.T.S., *Impact of product quality and demand evolution on EU refineries at the 2020 horizon : CO2 emissions trend and mitigation options*2008: CONCAWE.
5. Tabak, S.A., F.J. Krambeck, and W.E. Garwood, *Conversion of propylene and butylene over ZSM-5 catalyst.* AIChE Journal, 1986. **32**(9): p. 1526-1531.
6. Borges, P.P., R. Ramos; Lemos, M. A. N. D. A.; Lemos, F.; Védrine, J. C.; Derouane, E. G.; Ribeiro, F. Ramôa, *Light olefin transformation over ZSM-5 zeolites: A kinetic model for olefin consumption.* Applied Catalysis A: General, 2007. **324**(0): p. 20-29.
7. Corma, A.I.S., *Microporous and Mesoporous Solid Catalysts*, in *Catalyst for Fine Chemical Synthesis*, E.J. Derouane, Editor 2006, New York: John Wiley & Sons. p. 125-136.
8. Simpson, D., *Hydrocarbon reactivity and ozone formation in Europe.* Journal of Atmospheric Chemistry, 1995. **20**(2): p. 163-177.
9. Dunker, A.M.M., Ralph E.; Pollack, Alison K.; Schleyer, Charles H.; Yarwood, Greg, *Photochemical Modeling of the Impact of Fuels and Vehicles on Urban Ozone Using Auto/Oil Program Data.* Environmental Science & Technology, 1996. **30**(3): p. 787-801.
10. Schmidt, R.W., M. Bruce; Randolph, Bruce B., *Oligomerization of C5 Olefins in Light Catalytic Naphtha.* Energy & Fuels, 2008. **22**(2): p. 1148-1155.
11. Tabak, S.A., *Chem. Abstr.*, 1981. p. 95, 24233.
12. O'Connor, C.T., in *Handbook of Heterogeneous Catalysis*, W. VCH Verlagsgesellschaft mbH, Editor 1997. p. 2380.
13. Skupinska, J., *Oligomerization of a-olefins to higher oligomers.* Chem. Rev., 1991: p. 91, 613-648.
14. Al-Jarallah, A.M., Anabtawi, J. A., Siddiqui,M.A.B., Aitani, A.M., Al-Sa'doun, A.W. , Catal. Today, 1992. **14**: p. 1.
15. Minachev, K.M.D., A.A. , Russ. Chem., 1998. **47**: p. 1037.
16. Mehri Sanati, C.H.a.S.G.J., *Catalysis: Volume 14 (Specialist Periodical Reports)*. Vol. 14. 1999: Royal Society of Chemistry. 304.

17. Bellussi, G.M., F.; Calemma, V.; Pollesel, P.; Millini, R., *Oligomerization of olefins from Light Cracking Naphtha over zeolite-based catalyst for the production of high quality diesel fuel.* Microporous and Mesoporous Materials, 2012. **164**(0): p. 127-134.

18. Knifton, J.F., J.R. Sanderson, and P.E. Dai, *Olefin oligomerization via zeolite catalysis.* Catalysis Letters, 1994. **28**(2): p. 223-230.

19. Mantilla, A.T., F.; Ferrat, G.; López-Ortega, A.; Alfaro, S.; Gómez, R.; Torres, M., *Oligomerization of isobutene on sulfated titania: Effect of reaction conditions on selectivity.* Catalysis Today, 2005. **107–108**(0): p. 707-712.

20. Quann, R.J.G., Larry A.; Tabak, Samuel A.; Krambeck, Frederick J., *Chemistry of olefin oligomerization over ZSM-5 catalyst.* Industrial & Engineering Chemistry Research, 1988. **27**(4): p. 565-570.

21. O'Connor, C.T., *Oligomerization*, in *Handbook of Heterogeneous Catalysis*, H. G. Ertl, Knozinger and J. Weitkamp (eds). Editor 2008, VCH, Weinheim. p. 2854-2863.

22. Bjørgen, M., Lillerud, K. P., Olsbye, U., Bordiga, S., Zecchina, A. , J. Phys. Chem. B, 2004. **108**: p. 7862.

23. Geobaldo, F., Spoto, G., Bordiga, S., Lamberti, C., Zecchina, A. , J. Chem. Soc., Chem. Commun., Faraday Trans. 1997. **93**: p. 1243.

24. Chen, C.S.H.B., Robert F., *Shape-Selective Oligomerization of Alkenes to Near-Linear Hydrocarbons by Zeolite Catalysis.* Journal of Catalysis, 1996. **161**(2): p. 687-693.

25. Brouwer, D.M., *Reactions of Alkylcarbenium Ions in relation to Isomerization and Cracking of Hydrocarbons*, in *In Chemistry and Chemical Engineering of Catalytic Processes*, S. R., G. C. A., Eds, Editor 1980. p. 137-160.

26. Kustov, L.M., Borovkov, V.Y. and Kazanskii, V.B., *Study of ethylene oligomerization on Bronsted and Lewis acidic sites of zeolites using diffuse reflectance IR spectroscopy.* Stud. Surf Sci. Catal., 1984: p. 18, 241-247.

27. Kofke, T.J.G.G., R. J., *A temperature-programmed desorption study of olefin oligomerization in H-ZSM-5.* J. Catal., 1989: p. 115, 233-243.

28. Figueiredo, J.L., *Heterogeneous Catalysis: An overview*, in *Catalysis from Theory to Application*, M.M.P. José Luís Figueiredo, Joaquim Faria, Editor 2008, Coimbra University Press: Coimbra. p. 3-30.

29. Órfão, J.J.M., *Mechanisms and Kinetic in Heterogeneous Catalysis*, in *Catalysis from Theory to Application*, M.M.P. José Luís Figueiredo, Joaquim Faria, Editor 2008, Coimbra University Press: Coimbra. p. 55-104.

30. Pujado, P., Ward DJ., *Gasoline Components*, in *Handbook of petroleum processing*, P.P. Jones DSJ, editors, Editor 2006, Springer: New York, United States. p. 372-399.

31. Gates, B.C., *Catalysis by Ion-Exchange Resins*, in *Handbook of Heterogeneous Catalysis*, K.H. Ertl G, Schuth F, Weitkamp J, Editor 2008, Weinheim: Wiley-VCH Verlag GmbH. p. 278-285.

32. Aslam M, T.G., Zey EG., *Kirk-Othmer Encyclopedia of Chemical Technology*, J.W. Sons, Editor 1997.

33. Harmer, M.A., Sun, Qun, *Solid acid catalysis using ion-exchange resins.* Applied Catalysis A: General, 2001. **221**(1–2): p. 45-62.

34. Marchionna, M., Di Girolamo, Marco, Patrini, Renata, *Light olefins dimerization to high quality gasoline components.* Catalysis Today, 2001. **65**(2–4): p. 397-403.

35. Sharma, M.M., *Some novel aspects of cationic ion-exchange resins as catalysts.* Reactive and Functional Polymers, 1995. **26**(1–3): p. 3-23.

36. Gonçalves, F., Borges, LEP, Borges, CP., *Synthesis of ethyl acetate by coupling a heterogeneous catalytic system with a pervaporation unit.* Sep. Sci. Technol, 2004. **39**: p. 1485-500.

37. Jhung, S., Chang, Jong-San, *Trimerization of Isobutene Over Solid Acid Catalysts.* Catalysis Surveys from Asia, 2009. **13**(4): p. 229-236.

38. Coutinho, F., Souza, RR, Gomes, AS., *Synthesis, characterization and evaluation of sulfonic resins as catalysts.* Eur. Polym. J., 2004. **40**: p. 1525-32.

39. Yoon, J.W., Jhung, Sung Hwa, Chang, Jong-San *Trimerization of Isobutene over Solid Acid Catalysts: Comparison between Cation-exchange Resin and Zeolite Catalysts.* Bull. Korean Chem. Soc., 2007. **29**.

40. Silva, C.M., Lin, Zhi, Antunes, Bruno M., *Alkenes oligomerization using resin catalysts.* Fuel (Submitted), 2013.

41. Rahimi, N.K., R., *Catalytic cracking of hydrocarbons over modified ZSM-5 zeolites to produce light olefins: A review.* Applied Catalysis A: General, 2011. **398**(1–2): p. 1-17.

42. Chiche, B.S., E.; Di Renzo, F.; Ivanova, I. I.; Fajula, F., *Butene oligomerization over mesoporous MTS-type aluminosilicates.* Journal of Molecular Catalysis A: Chemical, 1998. **134**(1–3): p. 145-157.

43. Liu, S.L., G.; Liu, Z.; Sun, X., *Butene-2 Oligomerization to Heavy Olefins over ZSM-5 Zeolite.* Petroleum Science and Technology, 2009. **27**(15): p. 1653-1660.

44. Miller, S.J., *Olefin oligomerization over high silica zeolites.* Stud Surf. Sci. Catal., 1987. **38**: p. 187-197.

45. Guisnet, M.R.R., F., *Zeólitos, Um Nanomundo ao serviço da Catálise*, ed. F.C. Gulbenkian2004, Lisboa.

46. Ribeiro, M.F.F., A., *Fundamental Aspects in Zeolites Synthesis and Post-Synthesis Modification*, in *Catalysis from Theory to Application*, M.M.P. José Luís Figueiredo, Joaquim Faria, Editor 2008, Coimbra University Press: Coimbra. p. 107-144.

47. Marcilly, C., *Topics in Catalysis.* 2000. **13**: p. 357.

48. Peratello, S.M., M.; Bellussi, G.; Perego, C., *Olefins oligomerization: thermodynamics and kinetics over a mesoporous silica–alumina.* Catalysis Today, 1999. **52**(2–3): p. 271-277.

49. A. Corma, A.M., S. Pergher, S. Peratello, C. Perego, G. Bellussi, Appl. Catal A: General, 1997. **152**: p. 107.

50. G. Bellussi, M.G.C., A. Carati, F. Cavani, 1991, assigned to Eniricerche.

51. F. Cavani, V.A., 1991, assigned to Enichem Synthesis, Eniriche.

52. G. Bellussi, F.C., V. Arrigoni, R. Ghezzi, 1992, assigned to Eniricerche, Enichem Synthesis, Snamprogetti.

53. B. Chiche, E.S., F. Di Renzo, I. I. Ivanova, F. Fajula, J. Mol. Catal. A: Chemical, 1998. **134**: p. 145.

54. G. Bellussi, C.P., A. Carati, S. Peratello, E. Previde Massara, G. Perego, *Studies in Surface Science and Catalysis*, in *Zeolites and Related Microporous Materials: State of the Art* H.G.K. J. Weitkamp, H. Pfeifer, W. H¨olderich (Eds.), Editor 1994, Elsevier. p. 85.

55. Catani, R.M., M.; Rossini, S.; Vaccari, A., *Mesoporous catalysts for the synthesis of clean diesel fuels by oligomerisation of olefins.* Catalysis Today, 2002. **75**(1–4): p. 125-131.

56. Klerk, A.D., Energy Fuels 20, 2006: p. 1799.

57. Marcilly, C., *Catalyse Acido-basique Application au Raffinage.* 2003. **2**: p. 475–506.

58. De Klerk, A.L., D. O.; Prinsloo, N. M., *Butene Oligomerization by Phosphoric Acid Catalysis: Separating the Effects of Temperature and Catalyst Hydration on Product Selectivity.* Ind. Eng. Chem. Res., 2006: p. 45, 6127.

59. W. Keim, A.B., M. Roper, *Comprehensive Organometallic Chemistry: the Synthesis, Reactions and Structures of Organometallic Compounds*, F.G.A.S. G. Wilkinson, E. W. Abel (Eds.), Editor 1982: Pergamon Press, Oxford. p. 371.

60. Y. Chauvin, J.G., J. Leonard, P. Bonnifay, J. W. Andrews, Hydrocarbon Process., 1982. **61**: p. 110.

61. S. M. Harms, M.K., C. T. O'Connor,, Fuel Process. Technol., 1989. **21**: p. 231.

62. C. T. O'Connor, S.S., M. Kojima, *Catalysis and Adsorption by Zeolites*, in *Studies in Surface Science andCatalysis,*, H.P. G. ¨Ohlmann, R. Fricke (Eds.), Editor 1991, Elsevier: Amsterdam. p. 491.

63. Blauwoff, P.M.M., Gosselink, J.W.Kieffer, E.P., Sie, S.T. and Stork, W.H.J., *Zeolites as Catalysts in industrial processes.*, in *Catalysis and Zeolites. Fundamentals and Applications*, J.W.a.L.P. (eds.), Editor 1999, Springer-Verlag: Berlin. p. 509-512.

64. Dzikh, I.P., J.M. Lopes, F. Lemos, and F. Ramoa Ribeiro, *Transformation of light alkenes over templated and non-templated ZSM-5 zeolites.* Applied Catalysis A: General, 1999. **177**(2): p. 245-255.

65. Martens, J.A., R. Ravishankar, I.E. Mishin, and P.A. Jacobs, *Tailored Alkene Oligomerization with H-ZSM-57 Zeolite.* Angewandte Chemie International Edition, 2000. **39**(23): p. 4376-4379.

66. J.S. Jung, J.W.P., G. Seo, *Appl. Catal. A: Gen. 288.* 2005: p. 149-157.

67. L. Wang, M.X., L. Tao, *Catal. Lett. 28.* 1994: p. 61-68.

68. Y. Yoshimura, N.K., T. Hayakawa, K. Murataa, K. Suzuki, F. Mizukami, K. Matano, T. Konishi, T. Oikawa, M. Saito, T. Shiojima, K. Shiozawa, K. Wakui, G. Sawada, K. Sato, S. Matsuo, N. Yamaoka, *Catal. Surv. Jpn. 4.* 2000: p. 157-167.

69. K. Wakui, K.S., G. Sawada, K. Matano, T. Hayakawa, Y. Yoshimura, K. Murata, F. Mizukami, *Catal. Lett. 84.* 2002: p. 259-264.

70. X. Wang, Z.Z., C. Xu, A. Duan, L. Zhang, G. Jiang, J., *Rare Earths 25.* 2007: p. 321-328.

71. K. Wakui, K.S., G. Sawada, K. Shiozawa, K. Matano, K. Suzuki, T. Hayakawa, K. Murata, Y. Yoshimura, F. Mizukami, *Stud. Surf. Sci. Catal. 125.* 1999: p. 449-456.

72. J. Lu, Z.Z., C. Xu, A. Duan, X. Wang, P. Zhang, J., *Porous Mater. 15.* 2008: p. 213-220.

73. K. Wakui, K.S., G. Sawada, K. Shiozawa, K. Matano, K. Suzuki, T. Hayakawa, Y. Yoshimura, K. Murata, F. Mizukami,, *Catal. Lett. 81.* 2002: p. 83-88.

74. Salbilla, D.L.K., K.; Sim, C.P.; Soyza, C.A., *Fluidized Catalytic Cracker Catalyst Selection: Equilibrium Catalyst Quality and Considerations for Selections.*

75. http://www.refiningonline.net/EngelhardKB/crep/TCR4_23.htm. *Effects of Rare Earth Oxides in FCC Catalysts*. 9/30/2010.

76. R.W. Hartford, M.K., C.T. O'Connor, *Ind. Eng. Chem. Res. 28.* 1989: p. 1748–1752.

77. Y. Wei, Z.L., G. Wang, Y. Qi, L. Xu, P. Xie, Y. He, *Stud. Surf. Sci. Catal. 158.* 2005: p. 1223–1230.

78. G. Zhao, J.T., Z. Xie, W. Jin, W. Yang, Q. Chen, Y. Tang, J. Catal., 2007. **248**: p. 29-37.

79. J. Wan, Y.W., Z. Liu, B. Li, Y. Qi, M. Li, P. Xie, S. Meng, Y. He, F. Chang, *Catal. Lett. 124.* 2008: p. 150-156.

80. Gates, B.C., *Catalytic Chemistry, Wiley Series.* 1992.

81. Hagen, J., *Industrial Catalysis: A Practical Approach, Wiley-VCH Verlag GmbH & CO.* 2006.

82. Sigma-Aldrich. *ASTM® D2887 Quantitative Calibration Mix*. Available from: http://www.sigmaaldrich.com/catalog/product/supelco/48882?lang=pt&region=PT.

83. International, Z. 2006 [cited 2013 February]; Available from: http://www.zeolyst.com/our-products/standard-zeolite-powders/zsm-5.aspx.

84. Microanalysis, E. *Quartz Wool Discs 16mm Diameter*. 2013 [cited 2013 March]; Available from: http://www.microanalysis.co.uk/product_details.php?prod_code=B1251&product=B1251.

85. Bronkhorst. *Mass Flow Controller*. 2012 [cited 2013 February]; Available from: http://www.bronkhorst.com/en/products/gas_flow_meters_and_controllers/elflow_select/.

86. Chemyx. *Syringe*. 2012 [cited 2013 February]; Available from: http://www.chemyx.com/products/nexus_syringe_pumps.html.

87. Equilibar. *Back Pressure Regulator (BPR)*. 2012 [cited 2013 February]; Available from: http://www.equilibar.com/back-pressure-regulator/product-details.asp.

88. DANI. *Fas Gas Chromatograph*. 2012 [cited 2012 December]; Available from: http://www.danispa.it/products.asp?products=Master%20GC%20Fast%20Gas%20Chromatograph.

89. TIF. *Combustible detectors*. April 2013]; Available from: http://www.tif.com/products/combustible_gas_detector_TIF8800A.

90. Rimmer, C., *E. Heftmann: Chromatography, 6th edition. Fundamentals and applications of chromatography and related differential migration methods. Part A: Fundamentals and techniques.* Analytical and Bioanalytical Chemistry, 2005. **382**(7): p. 1447-1448.

91. Tiako Ngandjui, L.M. and F.C. Thyrion, *Kinetic Study and Modelization of n-Butenes Oligomerization over H-Mordenite.* Industrial & Engineering Chemistry Research, 1996. **35**(4): p. 1269-1274.

92. Alberty, R.A., *Kinetics of the polymerization of alkenes on zeolites.* The Journal of Chemical Physics, 1987. **87**(6): p. 3660-3667.

93. Alberty, R.A., *Extrapolation of standard chemical thermodynamic properties of alkene isomer groups to higher carbon numbers.* The Journal of Physical Chemistry, 1983. **87**(24): p. 4999-5002.

94. Alberty, R.A.G., Catherine A. , *Standard Chemical Thermodynamic Properties of Alkene Isomer Groups.* Journal of Physical and Chemical Reference Data, 1985. **14**(3): p. 803-820.

95. Alberty, R.A.a.G., Catherine A., *Standard Chemical Thermodynamic Properties of Alkene Isomer Groups.* J. Phys. Chem. Ref. Data, 1985. **14**: p. 803-820.

96. Alberty, R.A., *Analytic expressions for equilibrium distributions of isomer groups in homologous series of alkanes, alkenes, and alkynes at a specified partial pressure of molecular hydrogen.* The Journal of Chemical Physics, 1990. **92**(9): p. 5467-5472.

97. O'Connor, C.T., *Oligomerization*, in *Handbook of Heterogeneous Catalysis*, H. G. Ertl, Knozinger and J. Weitkamp (eds). Editor 1997, VCH, Weinheim. p. 102, 323-362.

98. A. G. Oblad, G.A.M., H. Heinemann, in *Catalysis* P.H.E. (Ed.), Editor 1958, Reinhold: New York. p. 341.

99. S. J. Sealy, D.M.F., K. P. Moller, C. T. O'Connor, Chem. Eng. Sci., 1994. **49**: p. 3307.

100. Meintjes, K. and A.P. Morgan, *Chemical equilibrium systems as numerical test problems.* ACM Trans. Math. Softw., 1990. **16**(2): p. 143-151.

101. Laidler, K.J., Pure Appl. Chem., 1981. **53**: p. 753.

102. W. H. Press, B.P.F., S. A. Teukolsky, and W. T. Vetterling, , in *Numerical Recipes*1986, Cambridge University: New York.

103. Henrici, P., in *Essentials of Numerical Analysis with Pocket Calculator Demonstrations* 1982: New York.

104. Rodríguez, R.a.E., Juan J.; Coto, Baudilio, *Structural Characterization of Fuels Obtained by Olefin Oligomerization.* Energy & Fuels, 2009. **24**(1): p. 464-468.

105. Monteiro, A.L.S., Michèle Oberson; Souza, Roberto Fernando, *Low pressure ethylene oligomerization with a nickel-PÔ complex.* Polymer Bulletin, 1996. **36**(3): p. 331-336.

106. Fogler, H.S., *Elements of Chemical Reaction Engineering*. 3rd ed: LTC.

107. J. A. Martens, P.A.J., *Theorical Aspects of Heterogeneous Catalysis*, V.N.R. J. B. Moffat (Eds.), Editor 1992: New York. p. 52.

108. Freek Kapteijn, F.A.M., Jacob *Laboratory Catalytic Reactors: Aspects of Catalyst Testing*, in *Handbook of Heterogeneous Catalysis*, H. G. Ertl, Knozinger and J. Weitkamp (eds). Editor 2008, VCH, Weinheim. p. 2022.

109. VICI. *GC Valve applications*. [cited 2013; Available from: http://www.vici.com/support/app/app11j.php.

8. Appendix

8.1 Appendix A – Proposed Mechanism pathway

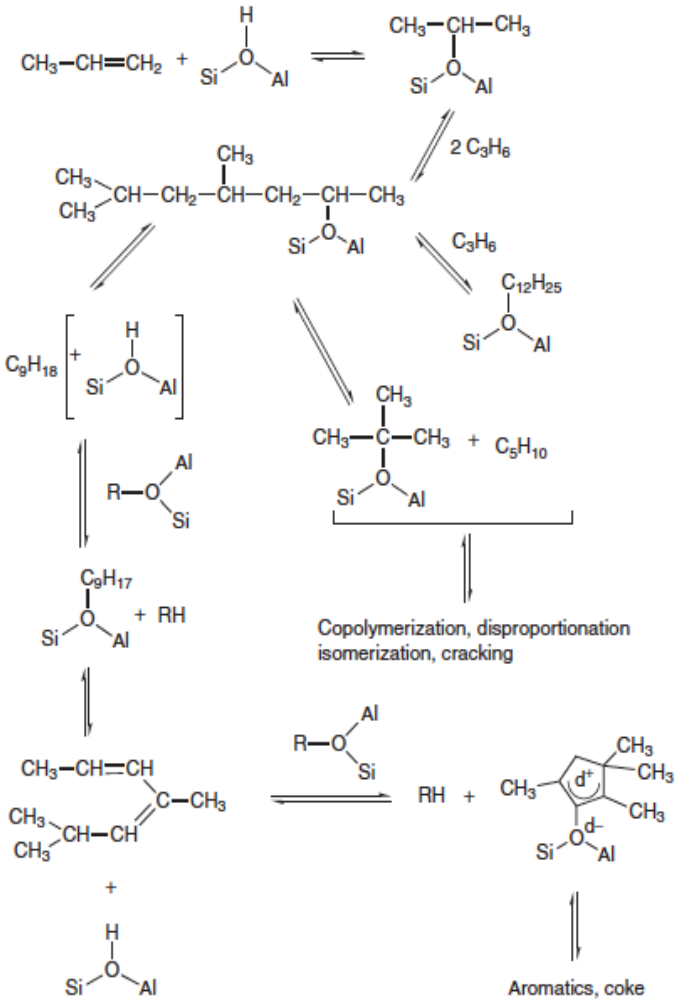

Figure 8.1 - Proposed mechanistic pathway for the oligomerization of propene by the literature [107]

8.2 Appendix B – Reactors Properties

Table 8.1 – Summary of relative reactor ratings (L = Low, M = Medium, H – High. Adapted[108]).

Aspect	Reactor type						
	PFR Differential fixed bed	PFR Integral fixed bed	PFR Solids transport (riser)	CSTR External recirculation	CSTR Internal fluid recirculation	CSTR Spinning catalyst basket	Batch Internal fluid recirculation
Ease of use	**H**	**H**	H	M - H	M	L - M	M
Ease of construction	**H**	**H**	L	M	M	L - M	M
Cost	**L**	**L**	H	L – M	M - H	M - H	M
Approach to ideal type	**M**	**H**	L	H	H	H	M
Approach to ideal type	**H**	**H**	M	H	M - H	L - M	H
Fluid-catalyst contact	**H**	**H**	M	H	M - H	L - M	H
Isothermicity	**H**	**M - H**	H	M - H	H	M	H
Temperature measurement	**H**	**H**	H	H	M - H	L	H
Kinetics	**H**	**H**	M	M	M - H	L - M	M
Deactivation noticed	**H**	**H**	L	M	M	M	L
GLS use	**L - M**	**M - H**	L	M - H	M - H	M	H

8.3 Appendix C – Different modes of the installation operation

Pure (olefin) atmospheric pressure

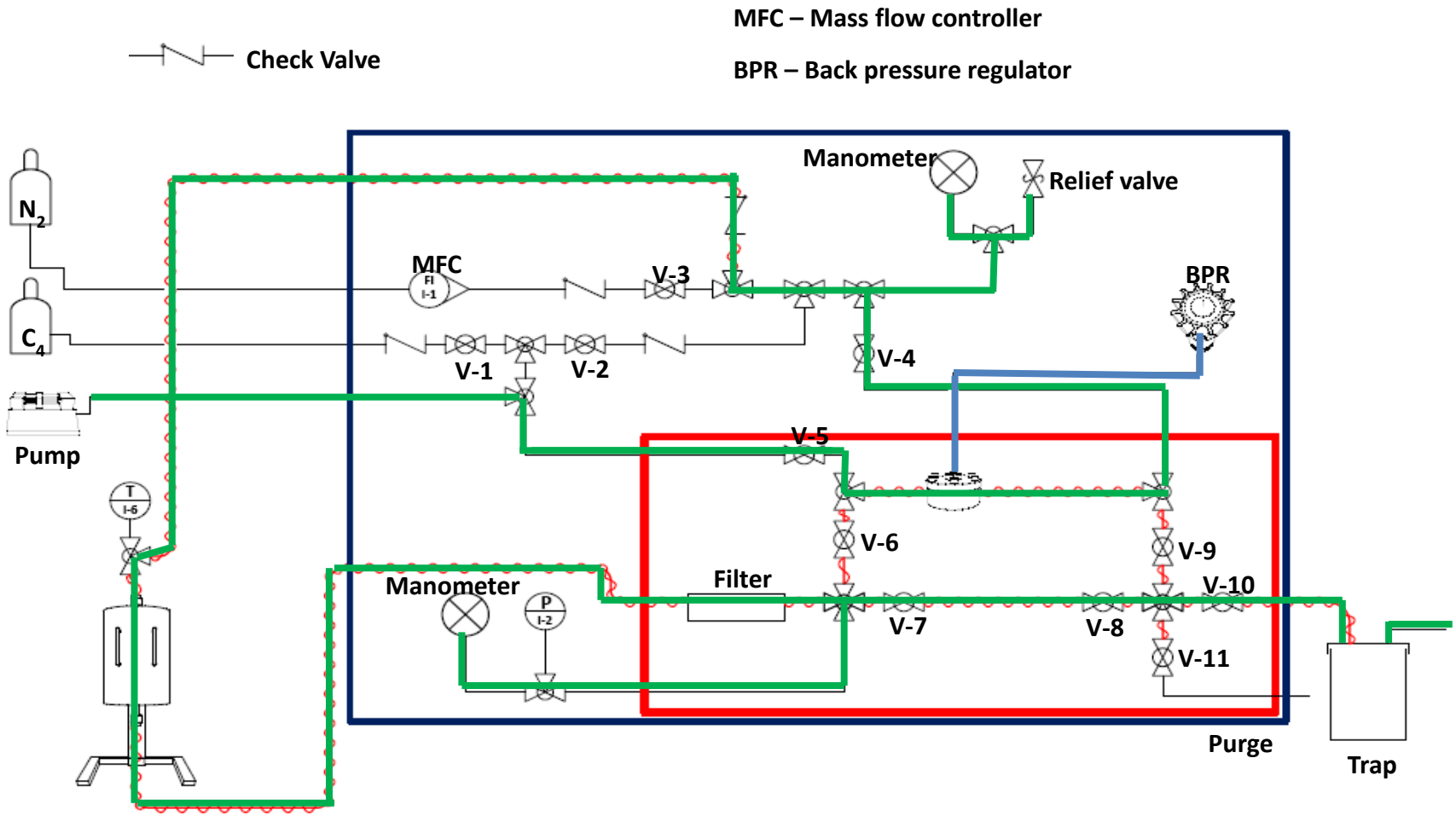

Figure 8.2 - Pure (olefin) atmospheric pressure schematic (open lines: ; heated line:).

Pure (olefin) high pressure

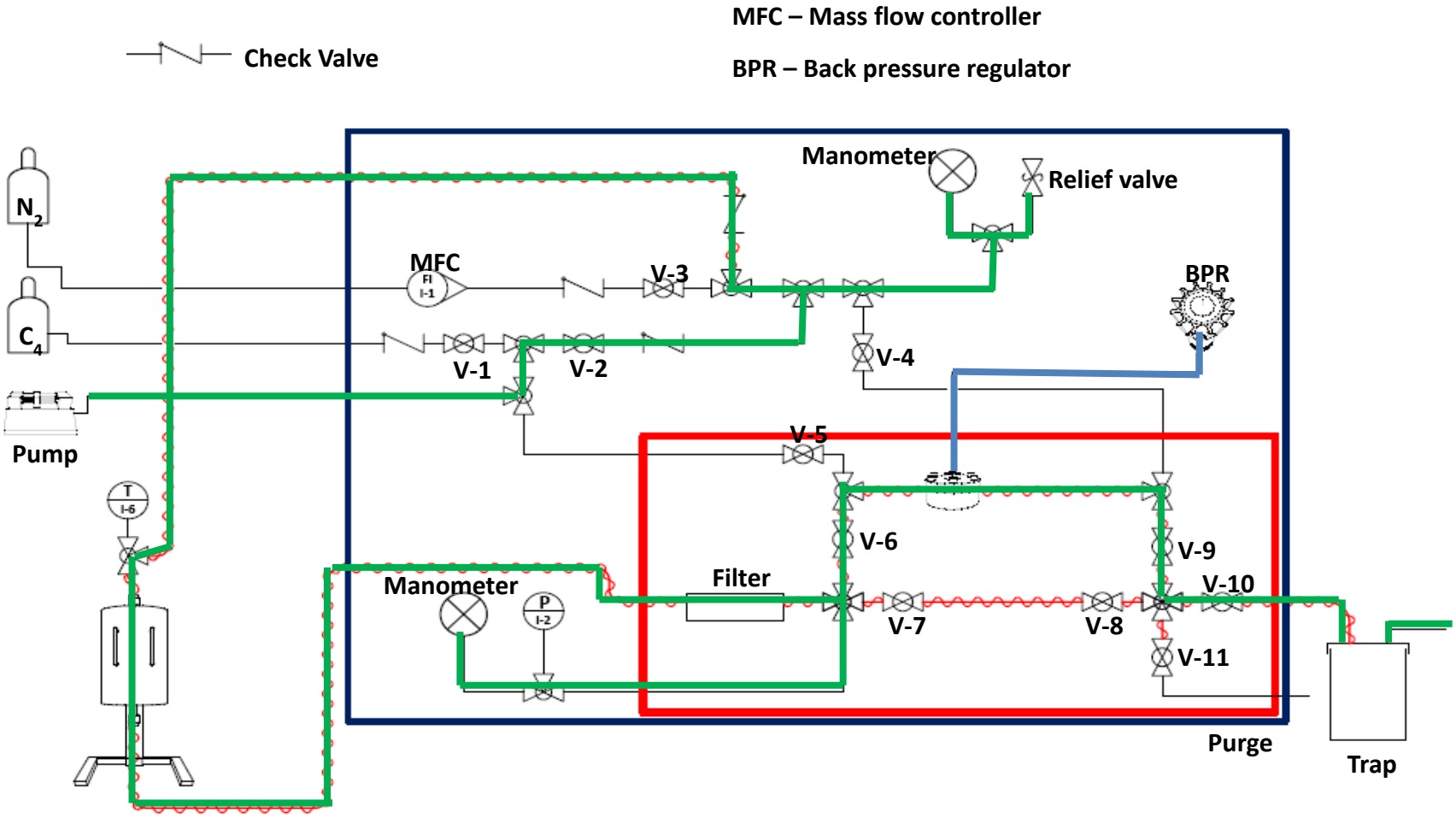

Figure 8.3 - Pure (olefin) high pressure schematic (open lines: ; heated line:).

Mixture (N_2/olefin) atmospheric pressure

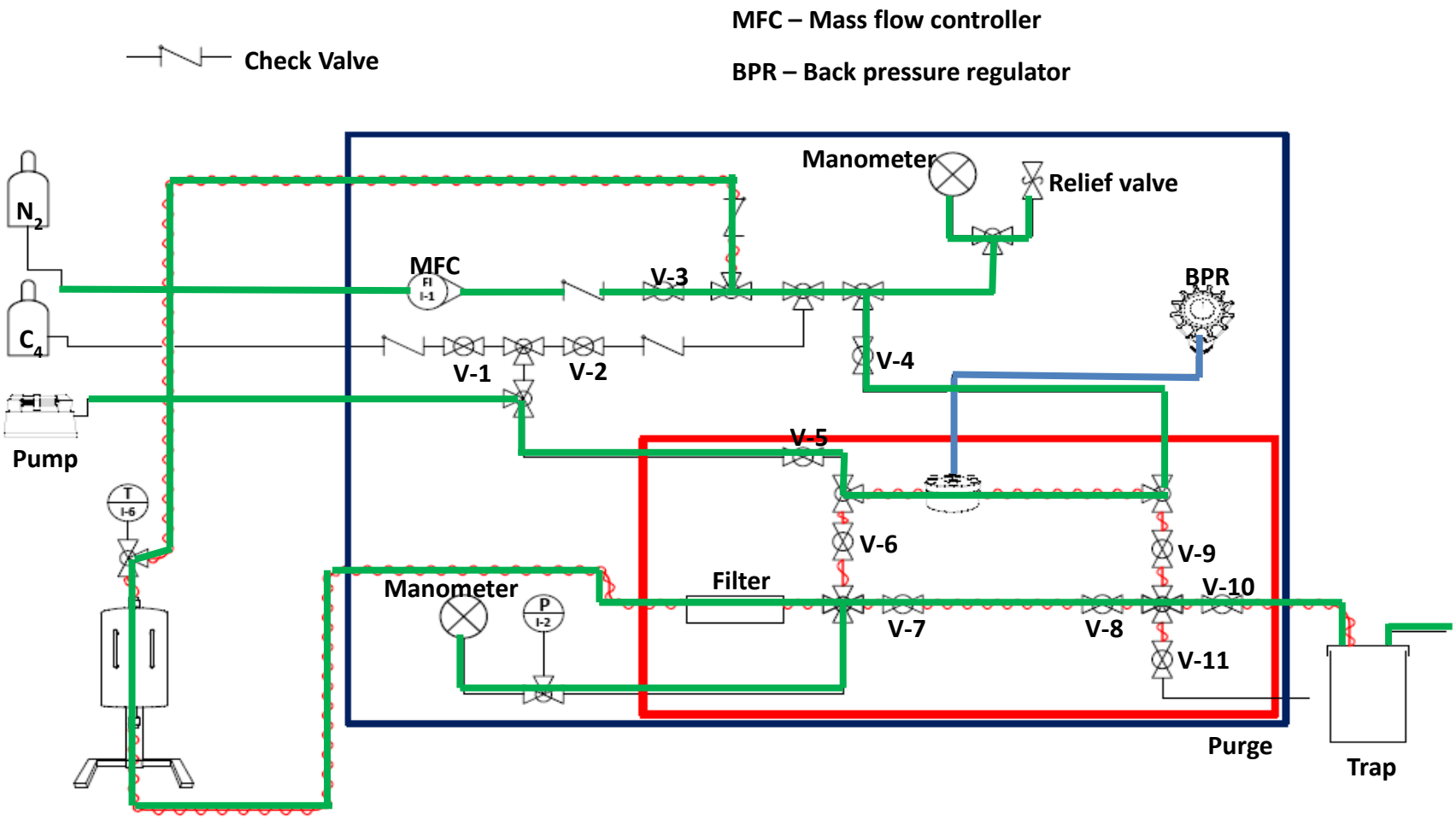

Figure 8.4 - Mixture (N2/olefin) atmospheric pressure schematic (open lines: ; heated line:).

Mixture (N_2/olefin) high pressure

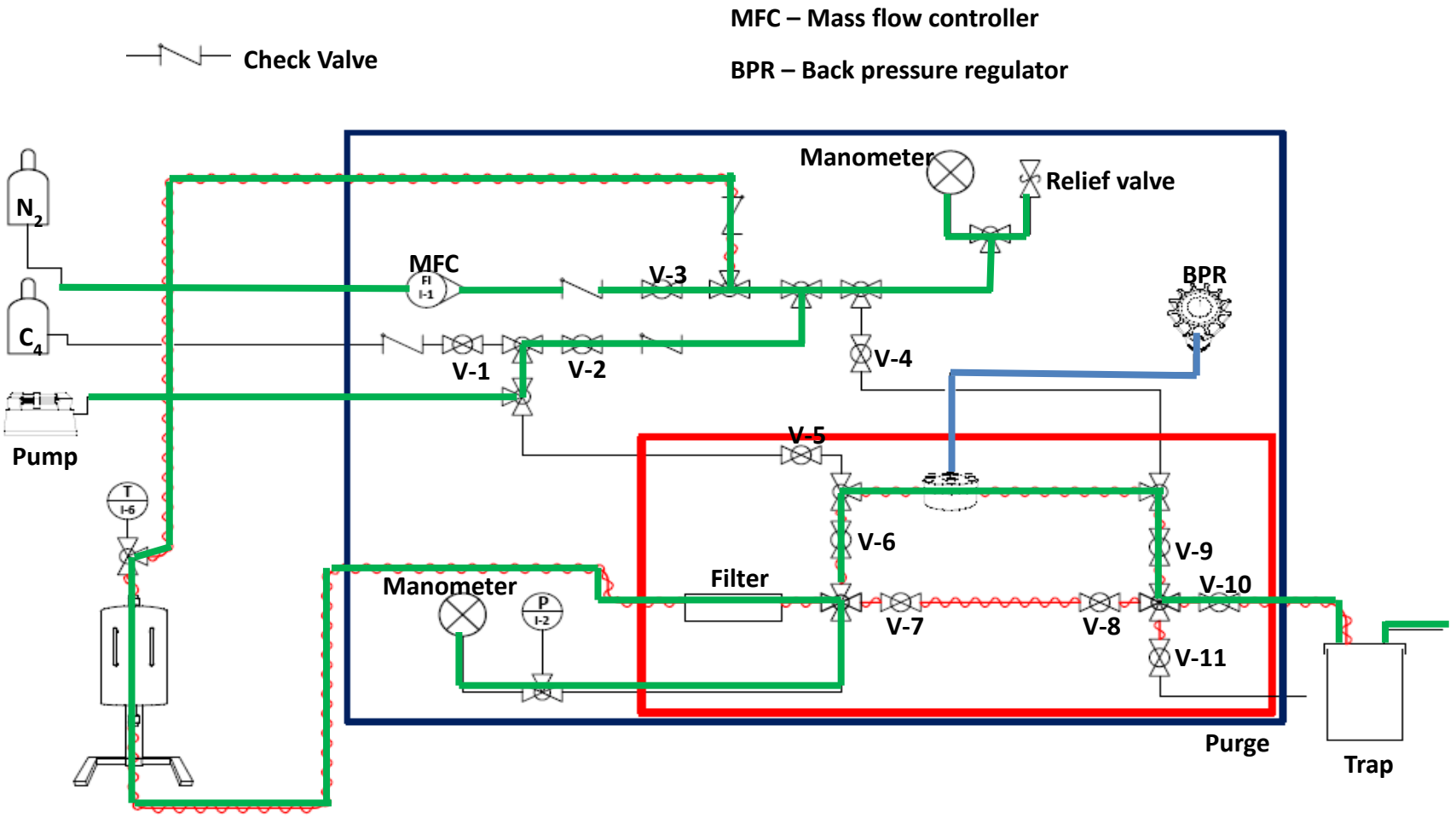

Figure 8.5 - Mixture (N2/olefin) high pressure schematic (open lines: ; heated line:).

Pre-treatment (N_2) atmospheric pressure

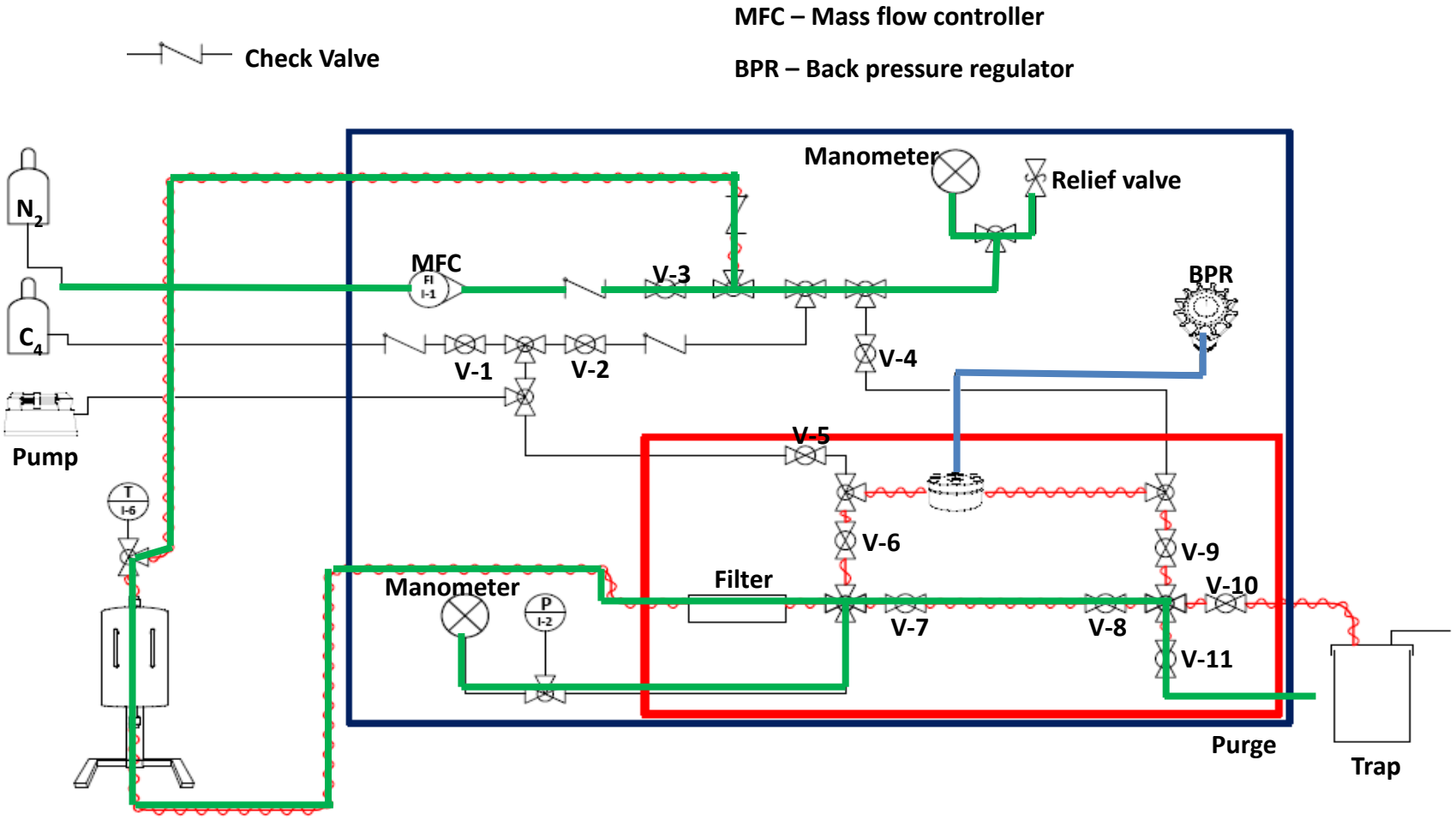

Figure 8.6 - Pre-treatment with nitrogen flow at atmospheric pressure schematic (open lines: ; heated line:).

8.4 Appendix D - Auxiliary Experimental Data

Table 8.2 - Auxilary experimental data.

Experiment	Loops (1^{st} to 11^{th}) min
1	30/30/30/30/30/30
2	30/30/30/30/30/15
3	30/30/30/30/30/30/30/30/30
4	5/10/15/30/30/30/30/30/30/30/59
5	5/10/15/30/30/30/30/30/30/30/60

8.5 Appendix E - Loop function

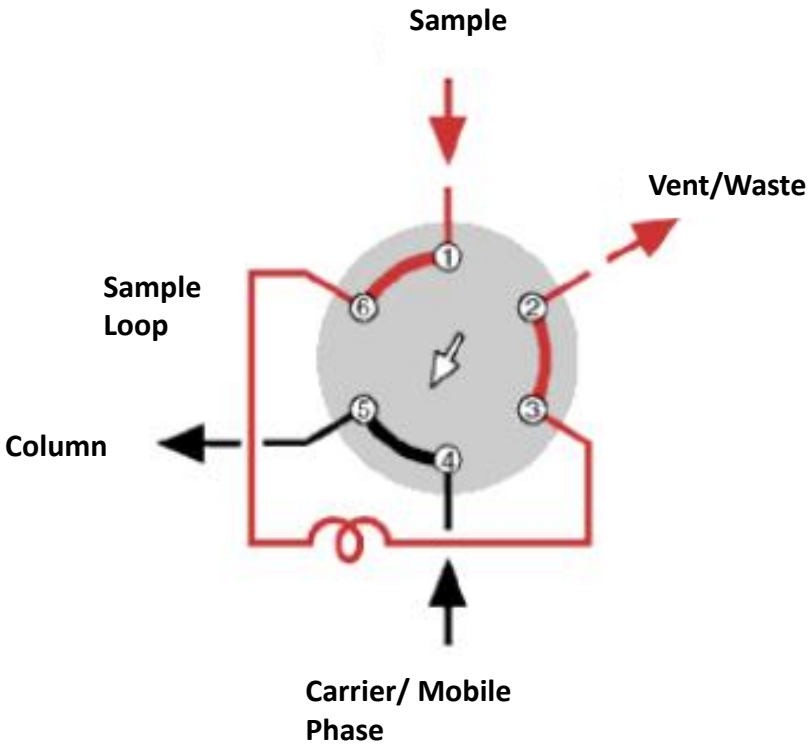

Figure 8.7 – Example of a load mode schematic (Position A) [109]**.**

With the valve in Position A, the sample flows through the external carrier flows directly through to the chromatographic column.

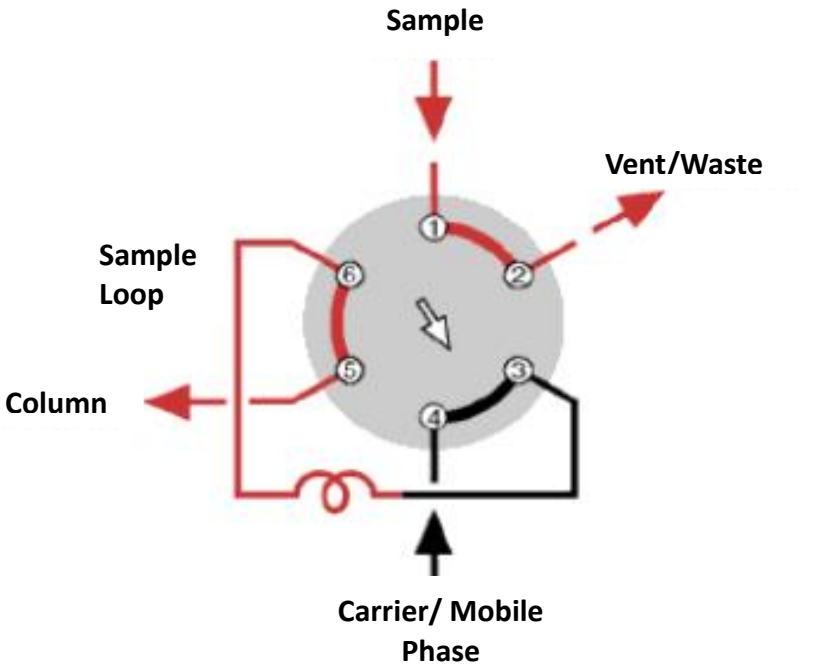

Figure 8.8 - Example of the inject mode schematic (Position B).

When the valve is switched to Position B, the sample contained in the sample loop and valve flow passage is injected into the column.